Utah State University

DigitalCommons@USU

All Graduate Plan B and other Reports | Graduate Studies

8-2018

Analysis of the Parkway Drive Landslide, North Salt Lake, UT

Brianna V. Hill
Utah State University

Follow this and additional works at: https://digitalcommons.usu.edu/gradreports

 Part of the Geology Commons, and the Geomorphology Commons

Recommended Citation

Hill, Brianna V., "Analysis of the Parkway Drive Landslide, North Salt Lake, UT" (2018). *All Graduate Plan B and other Reports*. 1311.
https://digitalcommons.usu.edu/gradreports/1311

This Report is brought to you for free and open access by the Graduate Studies at DigitalCommons@USU. It has been accepted for inclusion in All Graduate Plan B and other Reports by an authorized administrator of DigitalCommons@USU. For more information, please contact digitalcommons@usu.edu.



ANALYSIS OF THE PARKWAY DRIVE LANDSLIDE, NORTH SALT LAKE, UT

by

Brianna V. Hill

A research report submitted in partial fulfillment
of the requirements for the degree

of

MASTER OF SCIENCE

in

Applied Environmental Geosciences

Approved:

_____	_____
Dr. Tammy Rittenour	Dr. Joel Pederson
Major Professor	Committee Member
_____	
Dr. Carol Dehler	
Committee Member	

UTAH STATE UNIVERSITY
Logan, Utah

2018

Copyright © Brianna Hill 2018

All rights Reserved

ABSTRACT

Analysis of the Parkway Drive Landslide, North Salt Lake, UT

by

Brianna V Hill, Master of Science

Utah State University, 2018

Major Professor: Dr. Tammy Rittenour

Department: Geology

On August 5th, 2014, a hillside failed behind a North Salt Lake City, UT neighborhood moving 97,000 m^3 of material down slope and threatening several homes. Aerial Photography, Digital Elevation Models (DEM), geochemistry, rain gage and seismic data were used to test the influence of a number of contributing factors in this landslide failure. Aerial photographs available from 1993 to present were examined for signs of tension cracks suggesting impending ground motion, as well as documentation of human modification along the hillslope. Repeat DEM analysis of elevation and slope of the hillside before and after the slide were examined to characterize the pre-failure hillslope and subsequent landslide. Geochemical analyses were run on samples of the Tertiary Norwood Tuff within and outside of the landslide boundaries. Precipitation and seismicity data were collected and compiled to identify if they played a role in initiating the landslide.

Analyses indicate that the hillslope involved was previously part of a gravel pit in the 1990s, which was reclaimed for housing development in the early 2000s. Construction of homes, roads, and other building began in 2001 and continue to this day. Tension cracks began to appear along the slope by 2002, indicating downslope movement of unconsolidated material. DEM analysis reveals that the hillside was not at a critical angle for failure, suggesting that the linear, graded hillslope was stable prior to the landslide release. Geochemical analysis of a sample of altered (white) Norwood Tuff collected within the landslide boundaries indicated it is clay-rich, containing montmorillonite, an expandable clay mineral. Norwood Tuff is also found outside the affected slide area, but it was not altered to white clay. Precipitation data show a storm releasing 16 mm over one night, a typical precipitation total for the entire month of July, occurred six days prior to the landslide. Another large storm occurred the night before the slide. This could have provided the fluid for saturation of the montmorillonite clays in the altered Norwood Tuff underlying the landslide. No notable seismic events occurred leading up to the slope failure.

After the landslide event, the scarp and toe of the slide became over-steepened and the curvature of the toe increased. The toe is not stable and continued movement is expected and has been observed. The driving forces for this slide included human modification to the slope both during gravel pit operation and post reclamation construction that under-cut the toe of the hillslope and changed local hydrology of the area by decreasing infiltration above the slope. This was compounded by a large precipitation event that saturated the clay-rich material, which was the specific trigger for this landslide event.

ACKNOWLEDGMENTS

I would like to thank my boyfriend Michael for his love and support as I worked towards this degree. Knowing that there was always someone waiting for me after a long day of research was a huge comfort. The support and guidance from my committee members, Dr. Joel Pederson and Dr. Carol Dehler were crucial to the completion of this project and I couldn't be more grateful. I am also thankful to Kelly Bradbury and Andrew Lonero for their guidance as I dabbled in geochemistry work. Thank you to my family for supporting my decision to continue my education and for helping out financially when difficulties arose.

I would like to thank Emily Kleber, Ben Erickson, and Gregg Beukleman at the Utah Geological Survey for providing GPS and groundwater data to assist my research, and for providing insight to the geologic characteristics of the landslide, as well as the political issues surrounding the event. Thank you also to the USU Department of Geology for financial support so that I could collect samples and field images. Finally, I want to thank my advisor, Dr. Tammy Rittenour, for providing me the opportunity to complete my degree. Without your guidance and enthusiasm for this project, I'm not sure I could have succeeded. Thank you so much for believing in me, and pushing me to continue to work hard and explore new paths every day.

Table of Contents

Introduction……..1

Background……..3

Geologic Setting……...4

Landslide Initiation……..8

Previous Work…….8

Research Design…….11

Results and Discussion……..18

Concluding Observations and Comments…..……54

Works Cited……...61

List of Tables

Table 1: Elements of Research Design……..11

Table 2: Areas of the slide and lengths of cracks identified in Aerial Imagery…….24

Table 3: ICPMS Results……40

List of Figures

Figure 1: Location Map of Parkway Drive Landslide…….1

Figure 2: Regional Map of Wasatch Front……..4

Figure 3: Springhill and Parkways Drive Landslides……..6

Figure 4: Field Photos of Stratigraphy…..……7

Figure 5: Field Photos of Ground Cracks……..13

Figure 6: Aerial Imagery of Parkway Drive Landslide…….19

Figure 7: Landslide Extents and Ground Cracks Identified……..22

Figure 8: Ground Cracks and Crack length.……..25

Figure 9: Post Slide Extents……..26

Figure 10: Gravel Pit Map ...……..…...27

Figure 11: Modification Above Hillslope ……..……..28

Figure 12: Zonal Statistics ……..……..30

Figure 13: Elevation Change…….31

Figure 14: Slope Change……33

Figure 15: Field Photo of Landslide …….36

Figure 16: Sample Locations…….37

Figure 17: Field Photos of Samples……...38

Figure 18: Grain Size Distribution…….39

Figure 19: Percentage Grain size in Each Sample…….39

Figure 20: ICPMS Ratios……...41

Figure 21: XRD Results…….43

Figure 22: GPS Survey Results…….46

Figure 23: Mitigation efforts……..47

Figure 24: Precipitation Compilation……49

Figure 25: Precipitation and Tension Crack Length……..50

Figure 26: Precipitation Preceding Landslide……..……..51

Figure 27: Average Monthly Precipitation……51

Figure 28: Surface Drainage……..53

Figure 29: Precipitation vs. Groundwater……..55

Figure 30: Seismic Event Compilation…….…….56

Figure 31: Conceptual Landslide Model……57

ANALYSIS OF THE PARKWAY DRIVE LANDSLIDE, NORTH SALT LAKE, UT

INTRODUCTION

Before 6 am on the morning of August 5th 2014, a rumbling woke the families living along Parkway Drive in North Salt Lake City, Utah. This rumbling was the beginning of a landslide on the 32m-tall hillslope behind the homes. Families quickly evacuated their homes and crossed the street to watch as the land mass slumped and slid downslope, pushing one house off its foundation. Twenty-seven families were evacuated immediately, with seven families cautioned to stay away from their homes overnight as authorities waited for the land to stabilize. In the end, approximately 97,000 m^3 of material had moved, leaving an 18m-high head scarp on the rotational landslide. In addition to the house that was ripped off its foundation, a tennis court at the Eagleridge Tennis and Swim Club was severely damaged (Figure 1).

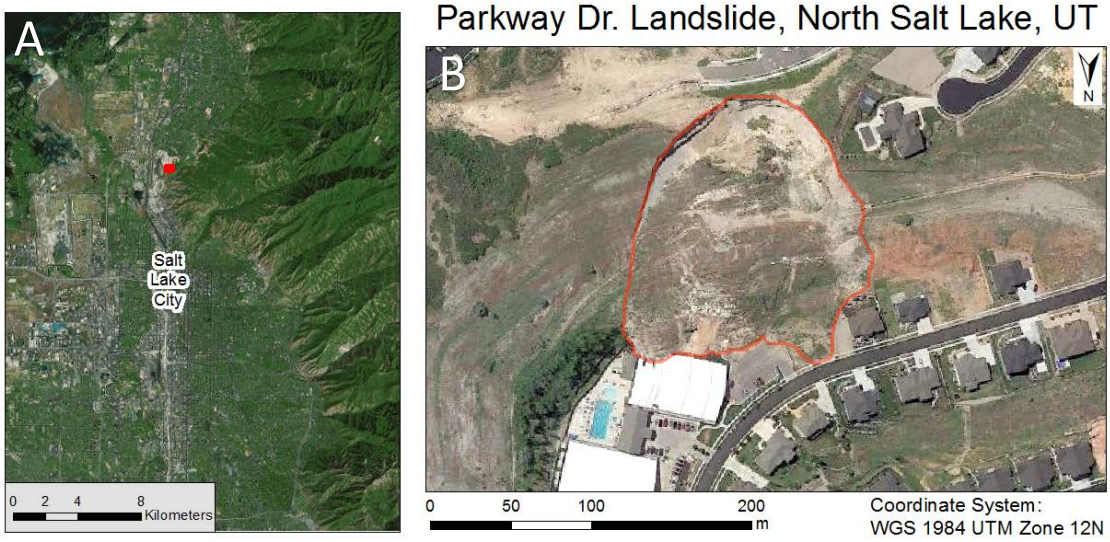


Fig. 1: (A) ESRI Map of the greater Salt Lake City metropolitan area in Utah with the location of the landslide as the red box. (B) Google Earth image of the Parkway Drive Landslide, taken in May 2015. The slide is outlined in red, and north is downward so the view is upslope.

Landslides are one of the most common natural hazards to affect urban communities. They are often difficult to predict because they are caused by a culmination of geologic, hydrologic and at times anthropogenic factors. Landslides cause significant property damage as well as loss of life in mountainous urban areas. The USGS estimates that landslides cause $1-$3 billion in damage and 25 – 50 deaths in the U.S each year (Highland & Bobrowsky, 2008; "Surveying Landslides in the U.S.," 2014). Globally, landslides cause thousands of deaths each year, particularly in developing countries due to increasing populations and limited assessment of natural hazards and restrictions on land development (Highland & Bobrowsky, 2008). With the increase in the spatial resolution of remote sensing techniques, landslide and other natural hazard maps have become easier to create and more freely available to landowners and communities. The more that landslide mechanics are studied and understood, the better job geologists and engineers can do to reduce landslide hazards.

This research was designed to investigate the conditions that led to the slope failure on Parkway Drive in North Salt Lake on August 5th 2014 and to test hypotheses related to the cause of slope failure. These include that failure was due to characteristics of the Quaternary geologic sediments and the bedrock geology underlying the slope, that failure was caused by rainfall events and hydrologic characteristics of the slope, that seismic shaking induced the failure, and/or that it was caused by human modification to the landscape.

BACKGROUND

Salt Lake City and its surrounding suburbs is along the Wasatch Front and is the largest urban area in the state of Utah with a population of approximately 1 million people (U.S. Census Bureau, 2010). The Parkway Drive landslide is in the Eaglepointe subdivision in North Salt Lake City, Utah (Fig.1). There have been over 2,500 new house construction permits issued in North Salt Lake since 1997, which includes all of the Eagle Point subdivision (U.S. Census Bureau, 2017). The neighborhoods surrounding Parkway Drive were an active gravel pit in the 1990s that was reclaimed and regraded for residential development which began in 2004-2008. Construction and development of the region continues to this day.

Some of the most desirable areas to live in the Salt Lake City Metropolitan area are along the mountain front on the highest terraces with pleasing views. However, in the case of the Eagle Point subdivision, engineered slopes created after reclamation efforts along these high benches are not as stable as undisturbed natural slopes. There have been two major landslides the North Salt Lake area, the Parkway Drive landslide and the Springhill landslide, an earthflow which initiated movement in 1998. The Parkway Drive landslide caused heavy property damage, but the Springhill landslide was detected before severe damage occurred, and the area was bought out and turned into a geologic park (Utah Geological Survey, n.d.). Since the initial failure of the Parkway Drive landslide in 2014, it has continued to reactivate and has threatened three more homes (Bowman, 2015). This project is focused on analyzing initial causes of this landslide in order to better anticipate future ground movement in this area.

GEOLOGIC SETTING

The Parkway Drive landslide is situated on the western flank of the Wasatch Mountains, a steep, normal-fault-bounded mountain front. The Wasatch Fault is part of the intermountain seismic zone at the eastern edge of the Basin and Range Province, and is a significant seismic threat to the area (Arabasz, Smith, & Richins, 1980) (Fig. 2). The Basin and Range Province covers approximately 800,000 km^2 and is within an extensional regime resulting in parallel ranges separated by large desert basins (Fenneman, 1928). Block faulting along the Wasatch Fault, a segmented normal fault extending 343 km from Malad City, Idaho south to Fayette, Utah, created the Wasatch Range on the eastern edge of the Great Salt Lake basin (Machette et al., 1991).

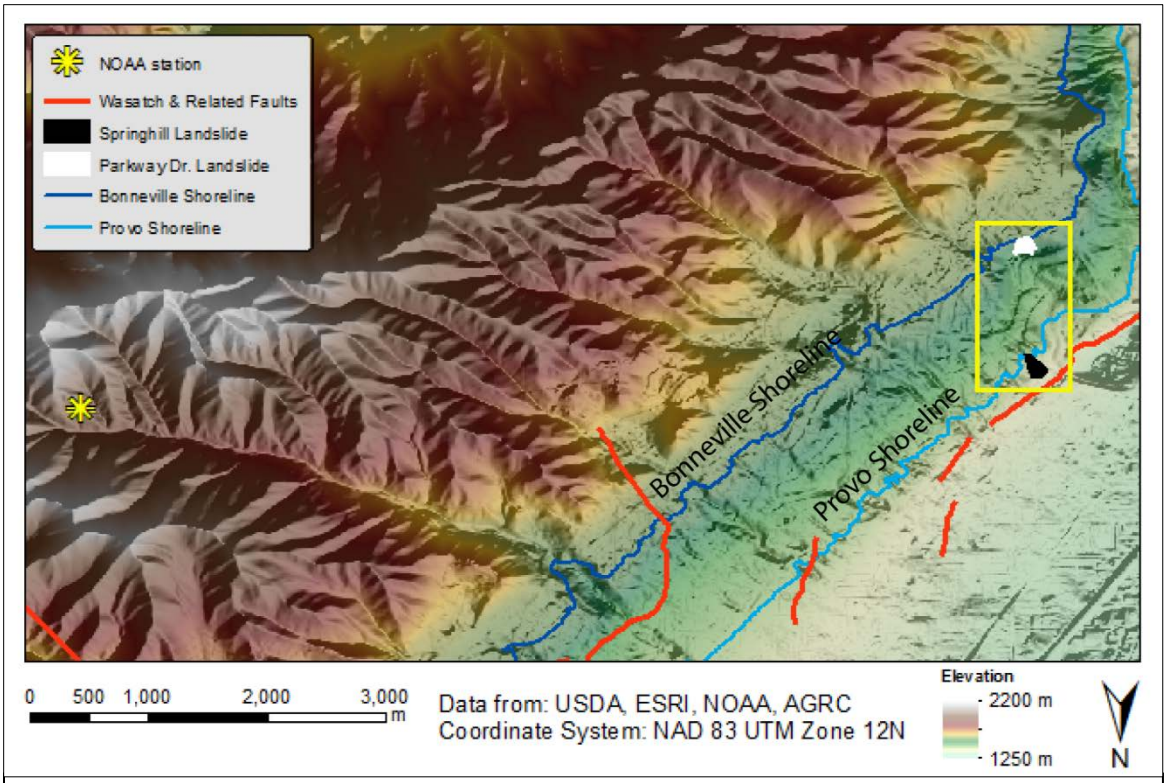


Fig. 2: Locations of the Parkway Dr. and Springhill Landslides in North Salt Lake, UT. The NOAA station used for climate data is approximately 6.2 km east of the landslide. The mapped sections of the Wasatch fault are shown in red, and the Bonneville and Provo Shorelines are shown in blue. The yellow box outlines the location of Figure 3.

A prominent feature of the landscape along the Wasatch Front are the lake shoreline terraces left behind by Lake Bonneville. Lake Bonneville formed during the last glacial epoch. It filled the Salt Lake basin and other interconnected valleys in northern Utah, reaching its highstand of ~1554 m above sea level at approximately 19 ka (Oviatt, 1997). This lake continued to fill until it passed its topographic threshold at Red Rock Pass and catastrophically flooded about 17.4 ka into the Snake River to the north. At that time, the lake level dropped to the Provo level at 1433 m above sea level (Oviatt, 1997).

The Parkway Drive landslide is located between the Bonneville and Provo shorelines, with the main head scarp cutting the Bonneville shoreline level. The sediments comprising the visible deposits are Pleistocene sand and gravels of the highstand of Lake Bonneville (Bryant, 1990). Unconsolidated sediments such as these are prone to slope failure as soon as the gradient surpasses a slope threshold (30-35°). The threshold for failure is decreased at higher pore water pressure (Rahn, 1969) (Fig. 3).

The Quaternary Bonneville shoreline sand and gravel deposits overlie a Tertiary volcanic unit, the Norwood Tuff which has a zircon-fission track age of 37.4 Ma (Horn, 1981) (Fig. 4). The Norwood Tuff is a volcanoclastic unit comprised of interbedded siltstone, sandstone, and ash layers. In the study area it is approximately 229 m thick (Horn, 1981). The Norwood tuff is exposed nearly continuously along the break in slope below the Bonneville shoreline due in part to human modification of the landscape. The Norwood Tuff has been associated with previous landslides in the area(Ashland, 2007; Beisner, Trandafir, & Bruhn, 2011; Trandafir & Amini, 2009). This tuff weathers to clay minerals

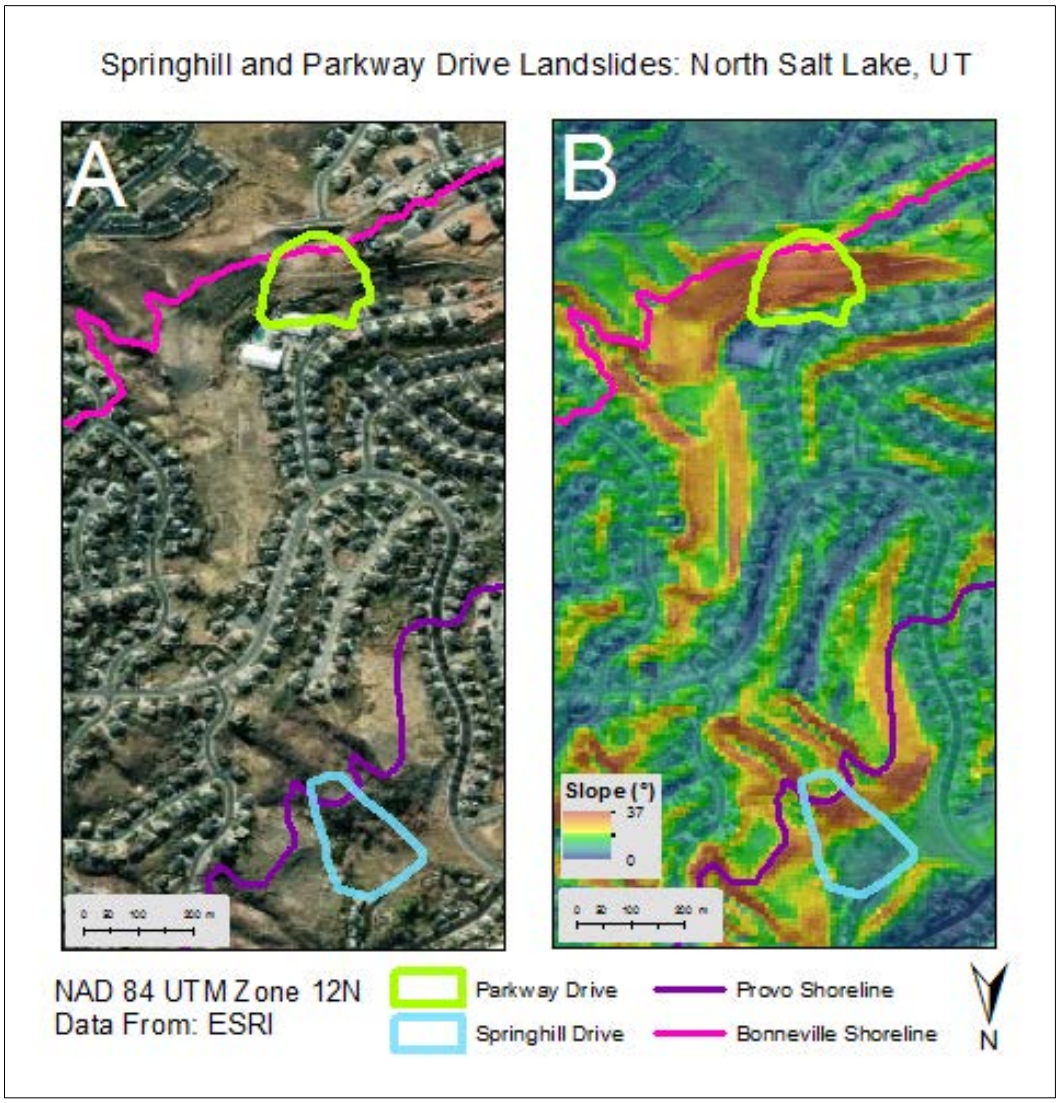


Figure 3: A) Location map of the Springhill Drive and Parkway Drive Landslides compared to the shorelines. B) Locations of the slides on a slope map based on a 2013 DEM, red is high slope, blue is low slope.

and has experienced hydrothermal alteration in the area. Dislodged blocks of bedrock along the slide body indicate that the Parkway Drive landslide initiated in the Norwood Tuff. Along the southern edge of the slide there is a contact between the white and reddish rocks and clays of the Norwood Tuff. Field observations indicate that the Springhill landslide is also associated with a white colored unit of the Norwood Tuff. One objective of this research will be to understand the differences between the white and red colored units of



Figure 4: Cross section of the slope that failed. This image is from construction work (digging a foundation) at the top of the landslide in 2018. A thin veneer of Bonneville gravels overlie a thick bed of Tertiary Volcanoclastic material of the Norwood Tuff unit. B shows a close up of the interbedded organic rich layers and colluvium.

the Norwood Tuff to determine if they have different geomechanical properties due to different mineralogy.

The juxtaposition of unconsolidated Bonneville Gravels overlying Tertiary volcanics along a steep mountain slope provides multiple dangers for landslides. Most likely the failure on August 5th 2014 was a result of some combination of the geomorphologic features, the weak bedrock, and human modification of the slope. The influence of precipitation and snowmelt, as well as regional seismicity, can create further instability on slopes. This research addresses the questions of how characteristics of the Quaternary geologic sediments and the bedrock geology underlying the slope, rainfall

events and hydrologic characteristics of the slope, seismic shaking, and/or that human modification to the landscape affected the stability of the hillslope.

LANDSLIDE INITIATION

Classical analysis of slope stability is based on the ratio of resisting forces to driving forces for a mass. This can be estimated using ae Factor of Safety equation, such as this simple one dimensional version:

$$FS = \frac{C + [\rho_s - (\rho_w\, m)]g\, z_s\, cos\Theta\, tan\Phi}{\rho_s\, g\, z_s\, sin\Theta}$$

Where C = soil cohesion, ρ_s = soil density, ρ_w = water density, m = proportion of soil that is saturated, g = gravitational constant, z_s = slab thickness normal to failure plane, Θ = failure plane angle above horizontal, and Φ = angle of internal friction for the given material. A FS = 1 means that the resisting forces are equal to the driving forces and therefore the slope is at the threshold for failure. Any value above 1 is considered safe, while values below 1 are considered dangerous. Hydrostatic pressure from water content reduces the friction (resisting forces), increases mass (driving), and can trigger slope failure at lower gradients (e.g. Iverson and Reid, 1992). Seismic activity could also be responsible for destabilizing a slope due to ground motion or liquefaction as grain to grain particle contact is reduced, and can cause failure.

PREVIOUS WORK

The Utah Geological Survey (UGS) has been monitoring the site since 2006 when initial ground cracks and slumps were observed. This monitoring expanded to formal GPS surveys and field photos after the 2014 landslide. Members of the UGS have shared

anecdotal evidence about potential triggers for this landslide. Their primary hypothesis is that 2014 was an abnormally wet year causing ground saturation, allowing the slope to fail. Another hypothesis involves the construction of a church on Eaglepoint Drive to the southeast of the slide and directly upslope; as sediments were excavate and dumped at the top of the slope, increasing the weight and driving forces, potentially making it more prone to failure.

The UGS has been actively monitoring the Parkway Drive landslide since its failure in 2014, mostly through repeat GPS surveys and piezometer monitoring of the shallow groundwater table. They placed approximately 15 steel beams in various locations surrounding and within the landslide boundaries and recorded a GPS location for each. Since that time, they have gone to the slide about two or three times a year to re-record the GPS locations of these beams. This has allowed a quantitative analysis of subsequent ground movement in different portions of the slide. They have published the results of these repeat surveys as maps on the UGS website (geology.utah.gov /hazards /landslides-rockfalls /parkway_drive_landslide/).

Two wells were drilled in to the main body of the slide, with data loggers to continuously record the piezometric level of the groundwater. This information allows the UGS to understand how the groundwater is flowing through the slide, and to alert them when higher groundwater levels may cause further slide dangers.

Since the slide occurred, the city of North Salt Lake has also sent out consultants and contractors to reclaim the slide area and mitigate future dangers. Based on evidence in aerial images and correspondence with the UGS, the main mitigation effort was to lower the slope by back-cutting the area to the south and above the main scarp to create a more

gradual slope. They also added boulders to the top part of the slope, at the base of the head scarp, in attempt to stabilize the sands and gravels that make up the surface cover above the Tertiary bedrock. Lastly, they added drains to gather water and pipe it away from the slope in an attempt to decrease groundwater pressure and prevent further loss of friction between sediment. Mostly, these attempts have been considered ineffective by the UGS and other researchers working on the slide. The lowering of the headscarp grade was effective, but adding boulders to the top half of the slide only adds mass to the upper slope. The drains focus on collecting overland flow and piping it away, but the main water in the affected sediment and poorly consolidated bedrock is in the subsurface, which has not been mitigated. In fact, a later reactivation of the lower section of the slide has disconnected the drain pipes (personal observation, Oct. 2017). The upper portion of the pipe can be seen above ground, and UGS researchers report that they rarely if ever see water flowing out of it.

The UGS is also monitoring other nearby landslides along the Wasatch front. The Springhill Drive landslide is within a kilometer of the Parkway Drive landslide, just downslope and to the north (Fig. 3). This slide has been creeping, rather than catastrophically failing like the Parkway Drive slide. The UGS also provides GPS surveys and groundwater monitoring at this slide. The mitigation effort at the Springhill slide was simply to buyout the cul-de-sac and renovate the area into a geologic park open for public recreation. Although of interest due to its proximity to the Parkway Drive landslide, the Springhill landslide will not be examined in the project due to the lack of pre- and post-movement imagery and elevation data.

RESEARCH DESIGN

This research was designed to test the importance of factors that led to the Parkway Drive landslide in North Salt Lake Utah. Potential factors include characteristics of the Quaternary geologic sediments and the bedrock geology underlying the slope, rainfall events and hydrologic characteristics of the slope, seismic shaking, and/or human modification to the landscape. To test the influence of these factors, aerial photography, repeat digital elevation models, and geologic maps were analyzed, and compared to field analyses and local rainfall and seismic data from the region. Four samples of altered Norwood Tuff were collected from the site for grain size, elemental, and mineral content analyses.

Data sources used to test hypothetical triggers include geologic maps, local precipitation and seismic stations, repeat air photo coverage, repeat Digital Elevation Models (DEMs), and geochemical analyses of different colored samples of the Norwood Tuff (Table 1). The influence of precipitation and seismic shaking were assessed by

Table 1: Elements of Research Design

Type	Source	Month/Years	Resolution	Analysis
Aerial Photography	Google Earth	6/17, 7/16, 6/15, 6/13, 6/10, 4/07, 12/06, 9/06, 6/05, 9/04, 8/03, 5/02, 10/97, 8/93	15 m	Landslide area differencing and land use observations
	National Agriculture Imagery Program	06/2014		
Light Detection and Ranging (LiDAR) DEM	Open Topography	2013	< 2 m	Elevation, slope, and volume differencing
Structure from Motion DEM	Utah Geological Survey	5/15		
Precipitation Data	National Oceanic and Atmospheric Administration (NOAA)	1956- present	daily	Time series trends
Seismic Data	University of Utah Seismic Station	2010 - present		

temporally comparing the initiation of the slide and subsequent movement to data from nearby meteorological and seismic stations.

Geologic Maps

I used the USGS Salt Lake City quadrangle map to determine the locations of contacts between the Quaternary Bonneville gravels and the underlying Tertiary volcanics (Horn, 1981).

Aerial Photography Interpretation

In order to determine how the landscape was modified before the 2014 landslide and how the landslide has moved afterward, I georeferenced 15 m scale aerial imagery from Google Earth for 2005, 2006, 2007, 2010, 2013, 2015, 2016, and 2017. To georeference the Google Earth images, I added four control points to the corners outlining the desired image in Google Earth and recorded the latitude and longitude in decimal degrees for each point. With these points in place, the image was then exported as a .jpeg. This file type can be opened in ArcMap. Using the WGS1984 coordinate system, I then used the georeferencing toolbar in ArcMap to add control points. These points were the same as the four corner points added in Google Earth, and they were referenced using the recorded latitude and longitude in decimal degrees. The georeferencing toolbar was also used to make slight adjustments if the images were not perfectly aligned.

One objective was to identify the location and changes in length of ground cracks on the hillslope. Resolution became an issue when deciphering these ground cracks in the landslide area, but the most obvious (and therefore the largest) were outlined for each year

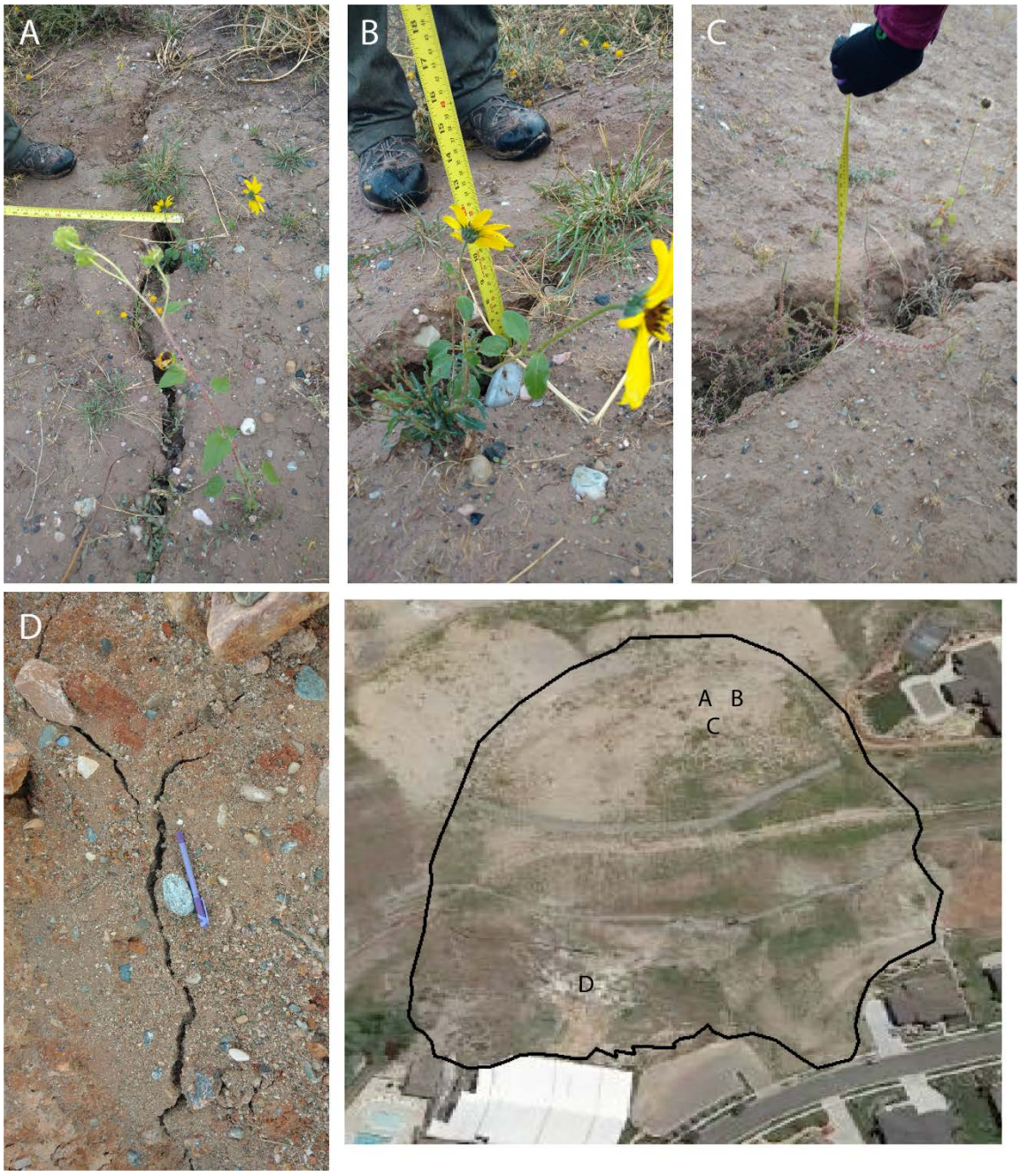


Fig. 5: Tension cracks identified on site in Oct. 2017. A, B, & C are located in the head of the slide, and D is located in toe of the slide.

except 2011 because the resolution was too low to identify any features with confidence. The 2017 image (including the extent of the slide and location of major ground cracks) was ground-truthed in early October when I assisted the Utah Geologic Survey (UGS) with GPS data collection at the site (Fig. 5).

In the 2014 image, I created a shapefile outlining the extent of the initial landslide to compare it to the preceding and successive images. I outlined the slide for each year, and subtracted subsequent shapefiles to create difference maps and calculate the lateral extent of the reactivation/creep each year. I also identified new ground cracks and slumps within the slide to detect new reactivated regions within the original slide and determine how they have changed over time. In the images prior to the 2014 landslide, I recorded any human interference to the landslide area (i.e. construction) as well as located any evidence for hillslope movement prior to the landslide. Any slumps or ground cracks noticed were outlined with shapefiles to compare to each successive year as well as to the main landslide in 2014. I also georeferenced two Google Earth images from the 1990s to show the extent of the gravel pit and compared the location of the gravel pit highwall created during max excavation to the location of the head scarp of the 2014 landslide.

Digital Elevation Model (DEM) Analyses

DEMs are used in determining slope stability and volumetric measurements in landscapes. Light detection and ranging (LiDAR) data exist from a survey flown in 2013 available through Open Topography, providing a pre-landslide data set for comparison. These data are a point cloud that was turned into a DEM with sub-1m resolution, by creating a surface based on the last returns from the LiDAR data.

Structure from motion (SfM) data exist from May, 2015. This is a point cloud of elevation data based of photography derived from a drone flight over the landslide performed by the Utah Geological Survey (UGS). Once again this was converted to a sub-1m resolution DEM for comparison to the landscape before the slope failure.

The point cloud data was turned in to a DEM using the software LAStools, developed by Martin Isenburg (Isenburg, 2007). This program allows an individual to upload point cloud data and select the desired returns, then interpolates the elevation values between the points to create a smooth surface. Once the DEMs were created, ArcGIS provided the tools to spatially calculate landscape attributes such as elevation and slope. These attributes were calculated and displayed as raster data. The raster calculator tool in GIS was used to difference rasters from pre- and post-slide data to spatially display the changes in the landscape ("How Raster Calculator works—Help | ArcGIS for Desktop," 2016). The specific changes were quantitatively calculated using the zonal statistics tools provided by ArcGIS.

Field Work, Sampling, and Geochemical Analyses

Four samples of the Tertiary Norwood Tuff were taken from within the landslide boundaries as well as from just outside the affected area. The samples analyzed include two from the more resistant, red-colored portions of the Norwood Tuff (outside the landslide boundary), and two from the less resistant, finer-grained, white portions of the exposed tuff within the slide. These samples were dried and then pulverized for ICPMS, X-ray diffraction, and grain-size analyses. Results from these analyses provided information on the differences in elemental composition, material content and grain-size

distributions. These data were used to determine if properties of the white colored portions of the Norwood Tuff are more susceptible to slope failure.

For Inductively Coupled Plasma Mass Spectrometry (ICPMS), the sample was dried and powdered. Then the sample was weighed out between 100-120 mg, and de-ionized (DI) water was added. The sample was then digested in 3.0 mL of 70% nitric acid and 5.0 mL of 48% hydrofluoric acid. After digestion the solution was diluted in DI water, and then analyzed on the Thermo XSeries 2 ICP-MS at the geochemistry laboratory in the Department of Geology at Utah State University. The analyses were run with a 10 millisecond dwell time using 25 sweeps for 4 replications of each sample. Calibration standard were run before and after the samples, and the correlation curve for each value had a coefficient of 0.999 or greater. The analyses were run by the lab manager, Andrew Lonero.

The dried and powdered samples were also analyzed using X-ray Diffraction analysis (XRD) at the X-ray laboratory in the Department of Geology at Utah State University. Powders were compacted into metal sample holders, and then analyzed using a Panalytical X'Pert Pro X-ray Diffraction Spectrometer. The analysis was run using 45 kV tension and 40 mA current, and measured diffraction patterns from $2\Theta = 2 - 75°$. The XRD peaks and profiles provide insight to the mineralogic compositions of the samples. Mineralogic interpretations were made using the X'Pert High Score software. Analyses were performed by Dr. Kelly Bradbury.

Representative sub-samples for grain-size analyses were collected from the same bulk samples used for ICP-MS and XRD analyses. Three to four subsamples from each bulk sample were analyzed on the USU Department of Geology's Malvern Mastersizer

2000 grain-size analyzer. The Malvern uses laser diffraction to calculate volumetric percent of grain-size classes between 0.01 -1000 µm. Three measurements were made from each subsample (n=9 measurements per sample). These data were combined to calculate the average grain-size percentages for each bulk sample.

The UGS completed a GPS survey of the landslide in October 2017. The UGS has approximately 16 GPS points that they repeat survey every few months in order to monitor the activity of the landslide and potentially predict any future failures. These survey results were compared with the DEM analyses to validate my methods.

The slide area has been modified to prevent future slides. Part of my field work was to record the mitigation attempts, and help identify areas where mitigation has been less effective.

Precipitation Analyses

The National Oceanic and Atmospheric Association (NOAA) records the precipitation over years for each of their monitoring stations. The City Creek Water Treatment Plant weather station is the closest precipitation station to the Parkway Drive landslide that recorded pre- and post-slide conditions. This station has recorded daily precipitation values since 1955. It is located 6.2 km east northeast of the landslide head scarp and approximately 1 km higher in elevation (Fig. 2). I examined daily precipitation data available from this station, and compiled the data extending back to 2000 in cumulative monthly precipitation values. This compilation allowed for a comparison between ground movement and total precipitation.

Seismic Record

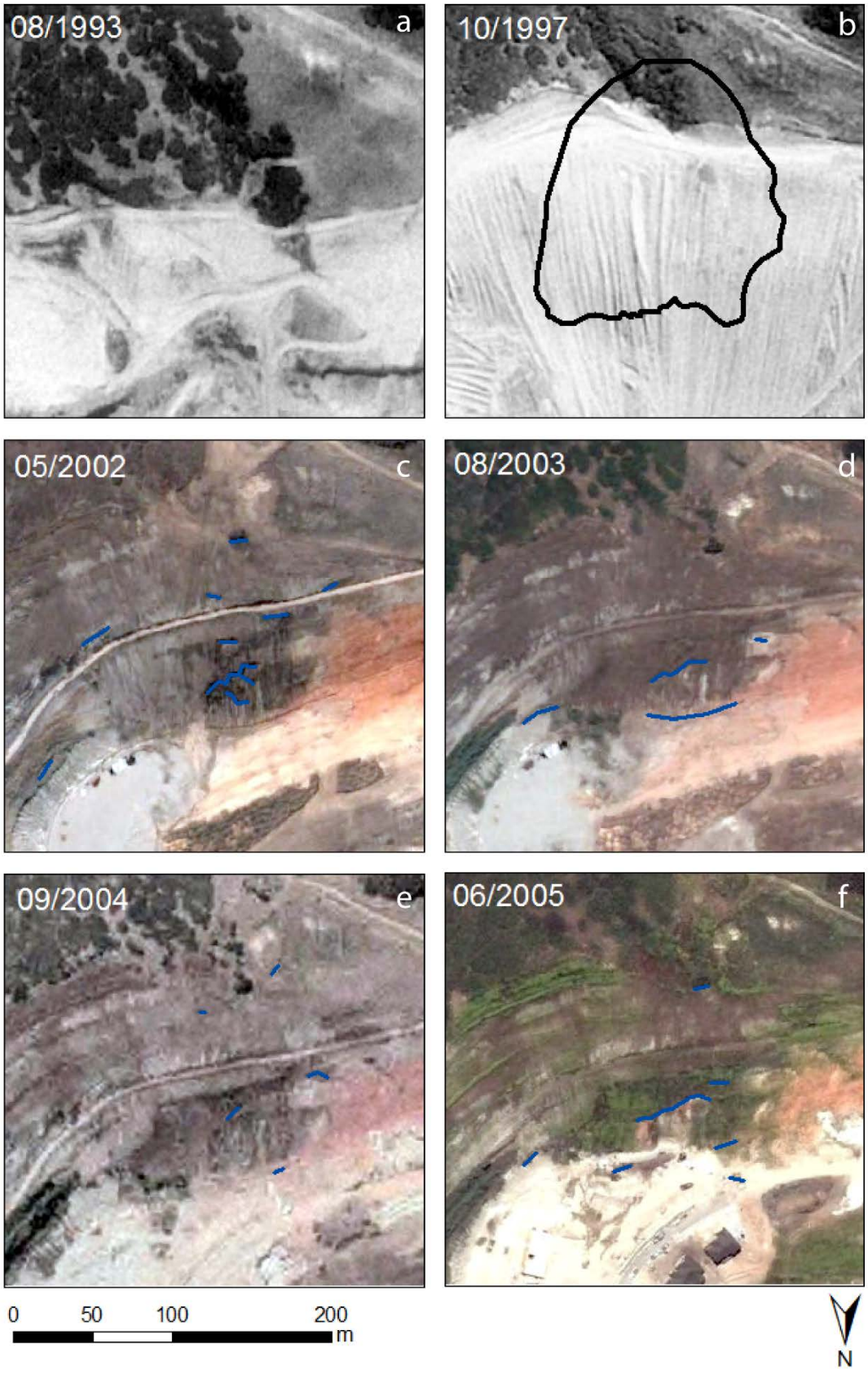
The University of Utah seismograph stations provide quarterly reports of Utah seismicity dating back to 2010. Daily data of ground shaking was compared to the lateral and volumetric motion of the slide to detect any temporal relationship between seismicity and slide motion.

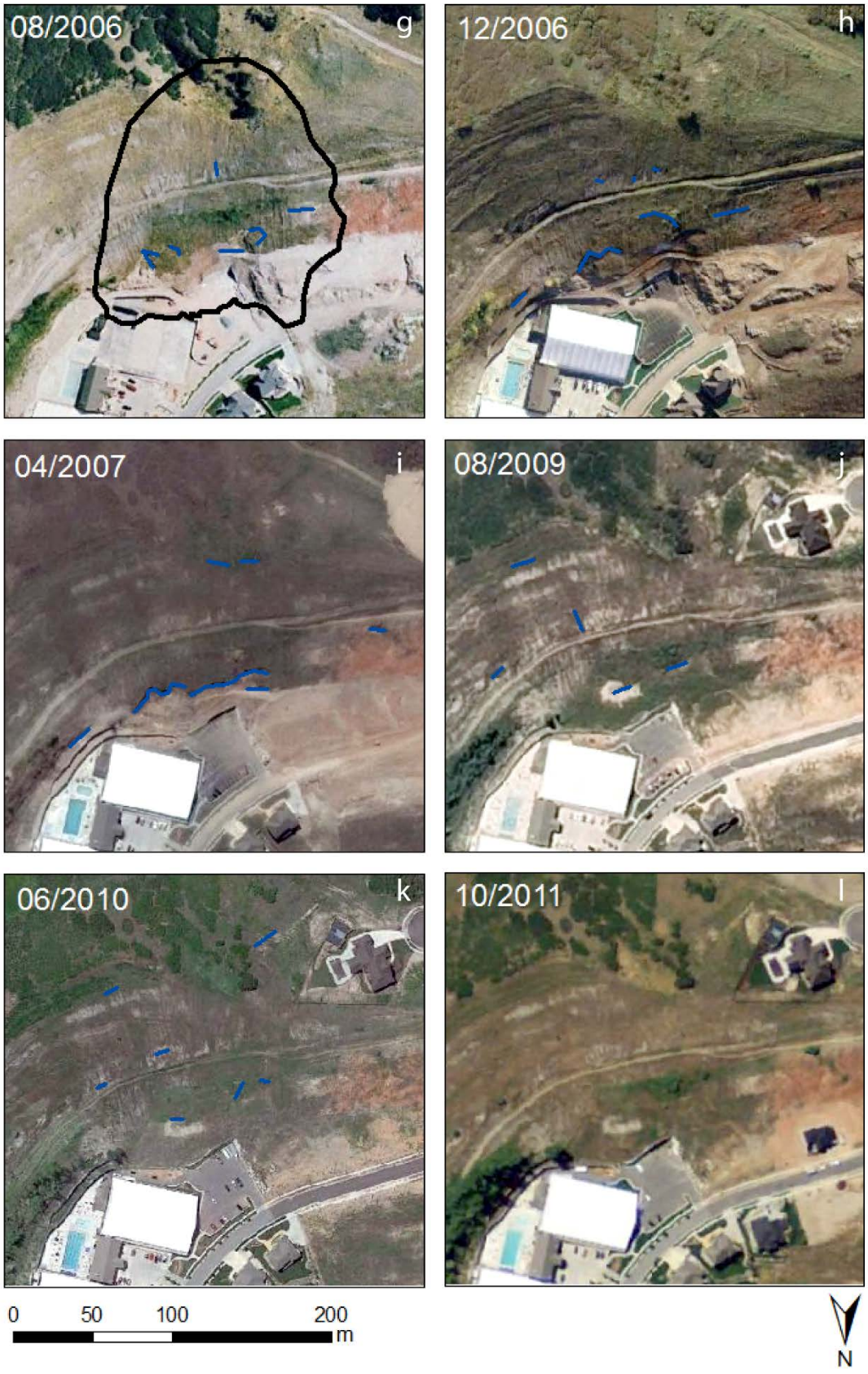
RESULTS AND DISCUSSION

Aerial Photography Interpretation

For this analysis I georeferenced and rectified each Google Earth image available between 1993 and 2017 (n=17) and created shapefiles outlining ground movement and tension ground cracks identified in each image (Fig. 6). The final GIS map created from the combined data are shown in Figure 7. While the number of fractures illustrated may be distracting to the viewer, the visual changes between images provides important context to understand the extent that this slope has been modified. The rate of crack annealment or growth for each month was calculated in ArcGIS (Table 2, Fig. 8). In the calculations, the area of reclaimed slope (4555 m^2) to the south of the head scarp was excluded as it was not a natural extension of the slide. The Google Earth imagery was used to calculate the aerial extent of the landslide and the number, location, and total length of extensional cracks.

Figure 9 illustrates the landslide lateral extents and tension cracks for the years following the major slide event. Between 2015 and 2016 the major lateral expansion of the slide area is due to reclamation efforts including the re-gradation of the slope. They did this by cutting back from the scarp up until they hit the road just south of the slide, lowering the angle of the headscarp from 75° to 36° by increasing its length. It makes sense that the


08/1993
a
10/1997
b
05/2002
c
08/2003
d
09/2004
e
06/2005
f
0
50
100
200
m
N


08/2006
g
12/2006
h
04/2007
i
08/2009
j
06/2010
k
10/2011
l
0
50
100
200
m
N

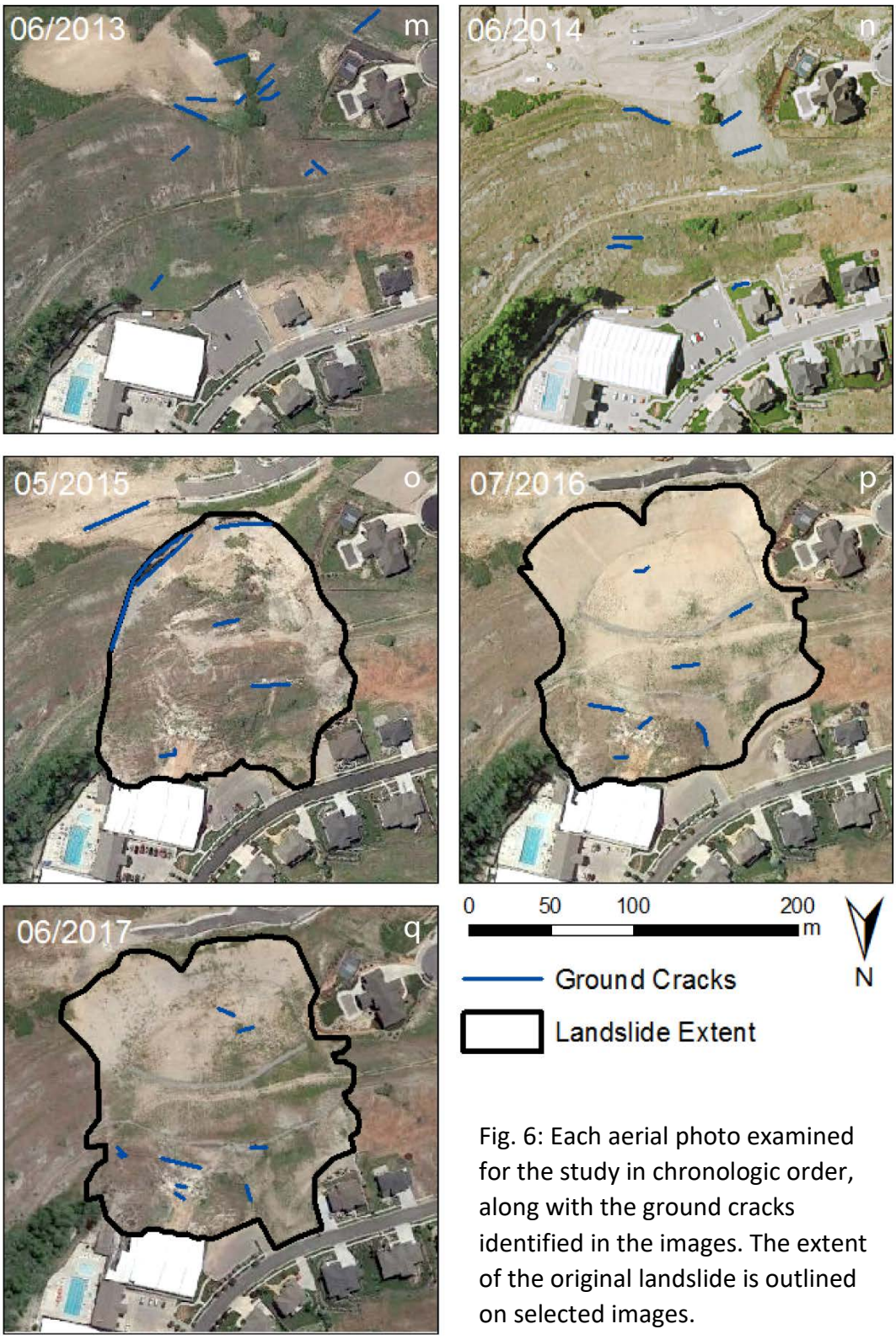


Fig. 6: Each aerial photo examined for the study in chronologic order, along with the ground cracks identified in the images. The extent of the original landslide is outlined on selected images.

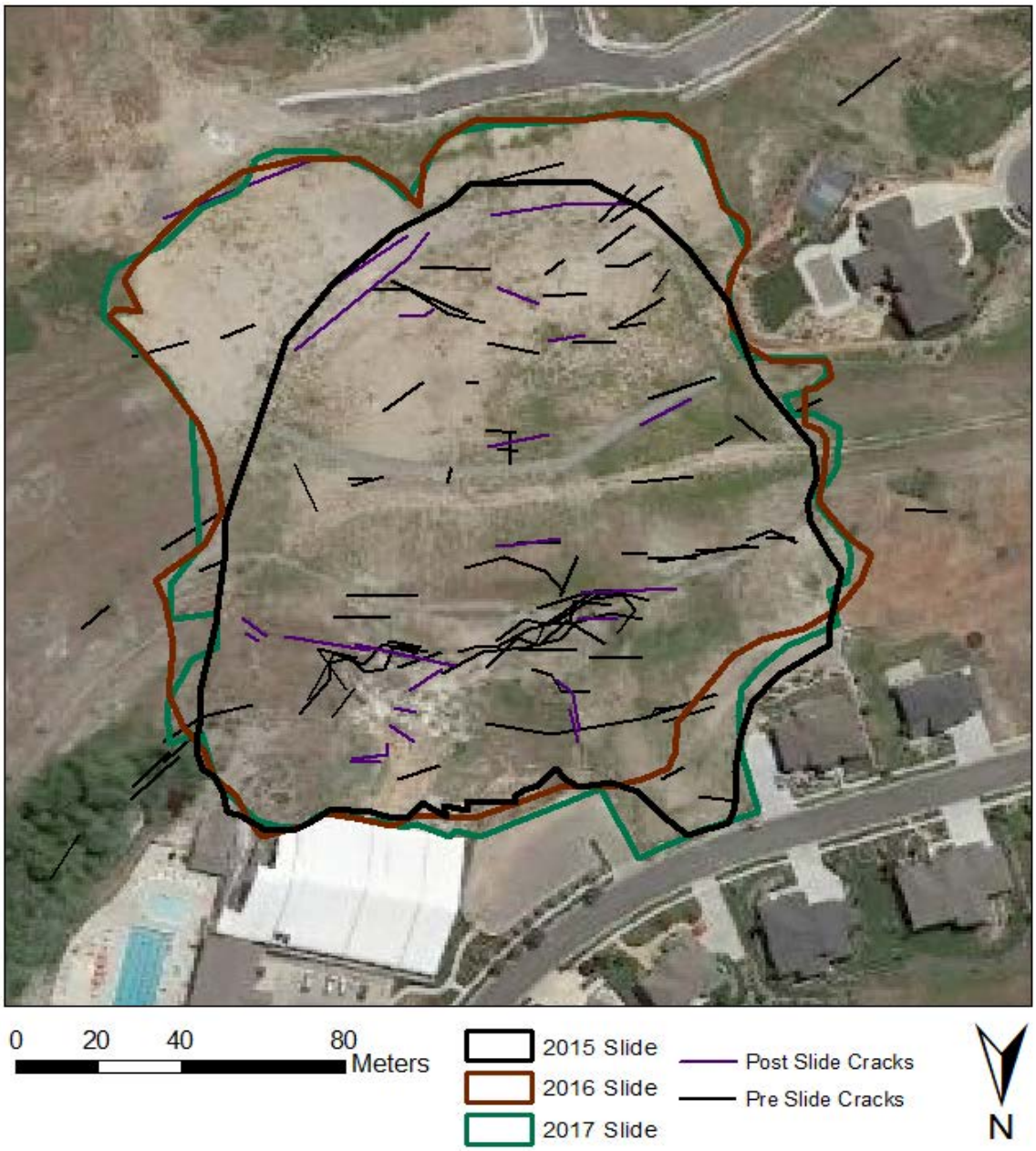


Fig 7: All landslide extents and grounds cracks identified using aerial photography. The cracks identified in images before Aug. 5th 2014 are shown in purple and those recognized in images later than Aug. 5th 2014 are green.

landslide did not expand greatly during this time because human activity was geared towards stabilizing the slope. Between 2016 and 2017 the slide extended laterally by 1071 m^2 due mainly to two areas of reactivation near the toe of the landslide, one on either side (Fig. 9). Material at the toe that has slid into the parking lots and building lots was removed during property maintenance.

The air photo analyses identified two periods of increased tension crack growth. These occurred during times of major construction in the area (Table 2, Fig. 8). In 2005-2007 the subdivision of Eaglepoint was being constructed. Air photos reveal that during this construction many of the removed materials were dumped along the head of what would later become the landslide.

DISCUSSION: The aerial photography analyses show that the hillslope that failed in the Aug. 5, 2014 landslide has been modified many times in the last 20 years. In the 1990s the area was covered by an active gravel pit, mining the Bonneville gravels (Fig. 6 & 10). The top of the gravel pit followed the Bonneville Shoreline and is coincident with the head scarp of the landslide.

Tension cracks with in the ground suggest instability of the hillslope immediately after the reclamation of the gravel pit. The ground cracks identified corroborate the DEM analyses that the areas that have the highest slope and highest change in slope are coincident to the areas with the largest clusters of ground cracks both before and after the landslide. By adding mass to the top of a slope, the downward forces are increased, and slope stability is lessened. Due to these changes in forces and stability, it is logical that more tension cracks would appear. The years leading up to and immediately following the slide have the largest increase in crack length (Table 2, Fig 8). This is logical because as aland mass begins to

Table 2: Areas of the slide and lengths of cracks identified in aerial imagery.

date	source	scale	landslide area (m^2)	added area from previous image (m^2)	# of cracks	crack length (m)	added length from previous image	crack annealment/ growth per month (m/months)
May-02	GE	15 m	N/A	N/A	10	155		
Aug-03	GE	15 m	N/A	N/A	4	127	-28	-1.9
Sep-04	GE	15 m	N/A	N/A	5	40	-87	-6.7
Jun-05	GE	15 m	N/A	N/A	7	116	76	8.4
Aug-06	GE	15 m	N/A	N/A	6	91	-25	-1.8
Dec-06	GE	15 m	N/A	N/A	8	116	25	6.3
Apr-07	GE	15 m	N/A	N/A	8	163	47	11.8
Aug-09	GE	15 m	N/A	N/A	5	60	-103	-3.7
Jun-10	GE	15 m	N/A	N/A	7	63	3	0.3
Oct-11	GE	15 m	N/A	N/A	N/A	N/A		
Jun-13	GE	15 m	N/A	N/A	6	102	39	1.1
Jun-14	NAIP	30 m	N/A	N/A	12	156	54	4.5
08/05/2015: Landslide!								
May-15	GE	15 m	19300	N/A	8	254	98	8.9
Jul-16	GE	15 m	23885	30	7	92	-162	-11.6
Jun-17	GE	15 m	24956	1071	9	88	-4	-0.3

GE = Google Earth

NAIP = National Agriculture Imagery Program

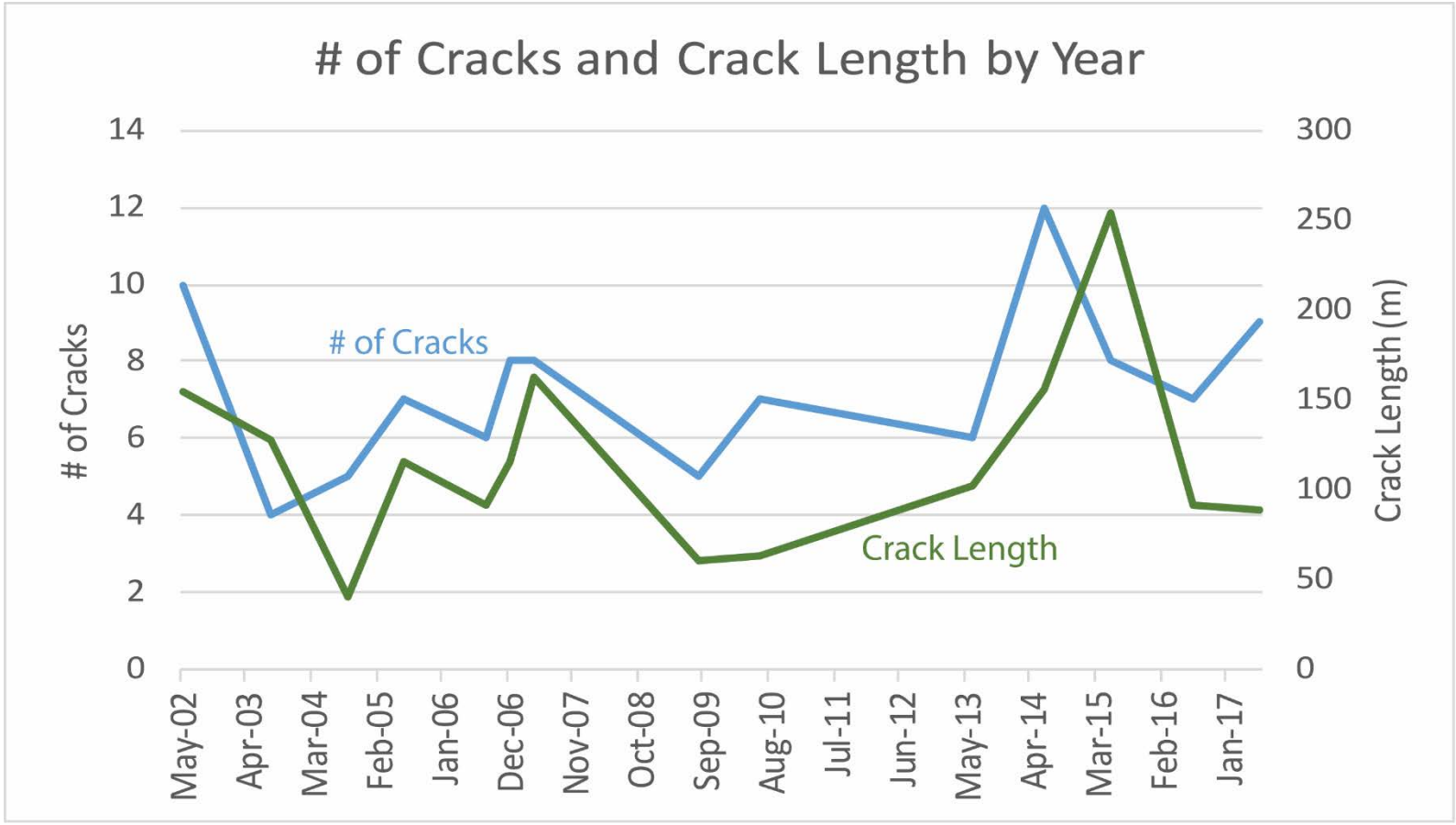


Figure 8: Number of cracks and Crack length plotted sequentially based on values from Table 2.

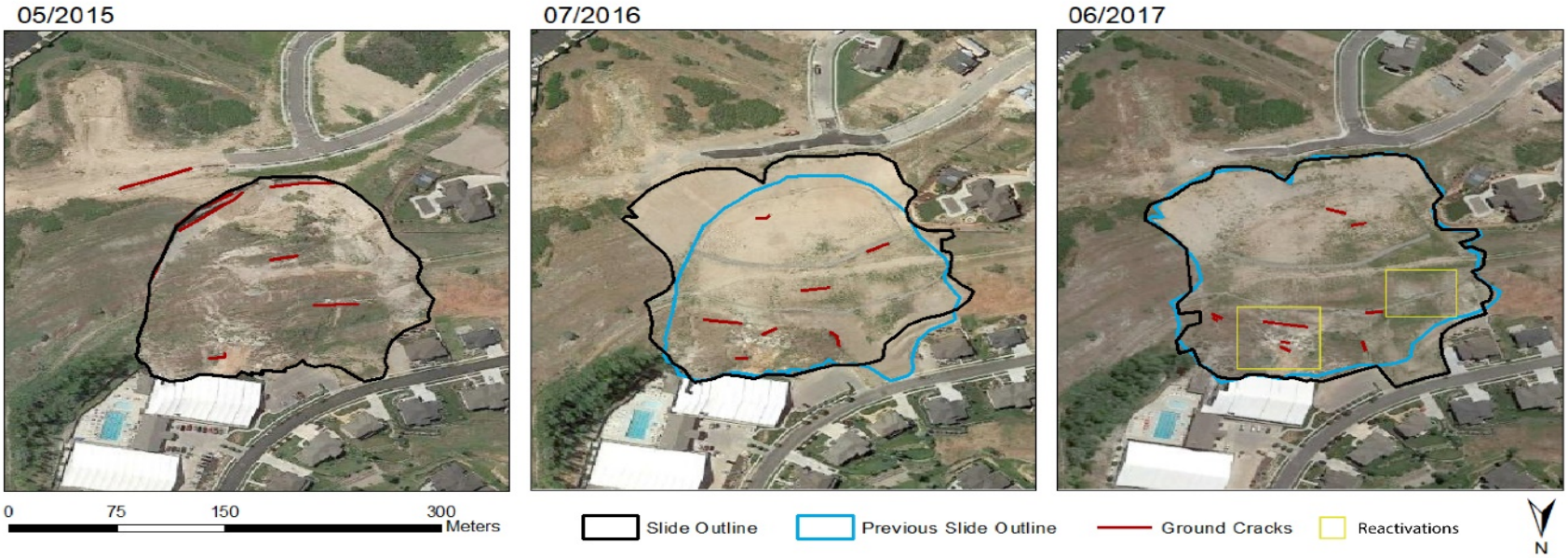


Fig. 9: landslide extents and identified ground cracks in images after the landslide occurred. The head of the slide was extended back to reduce the overall slope.

.

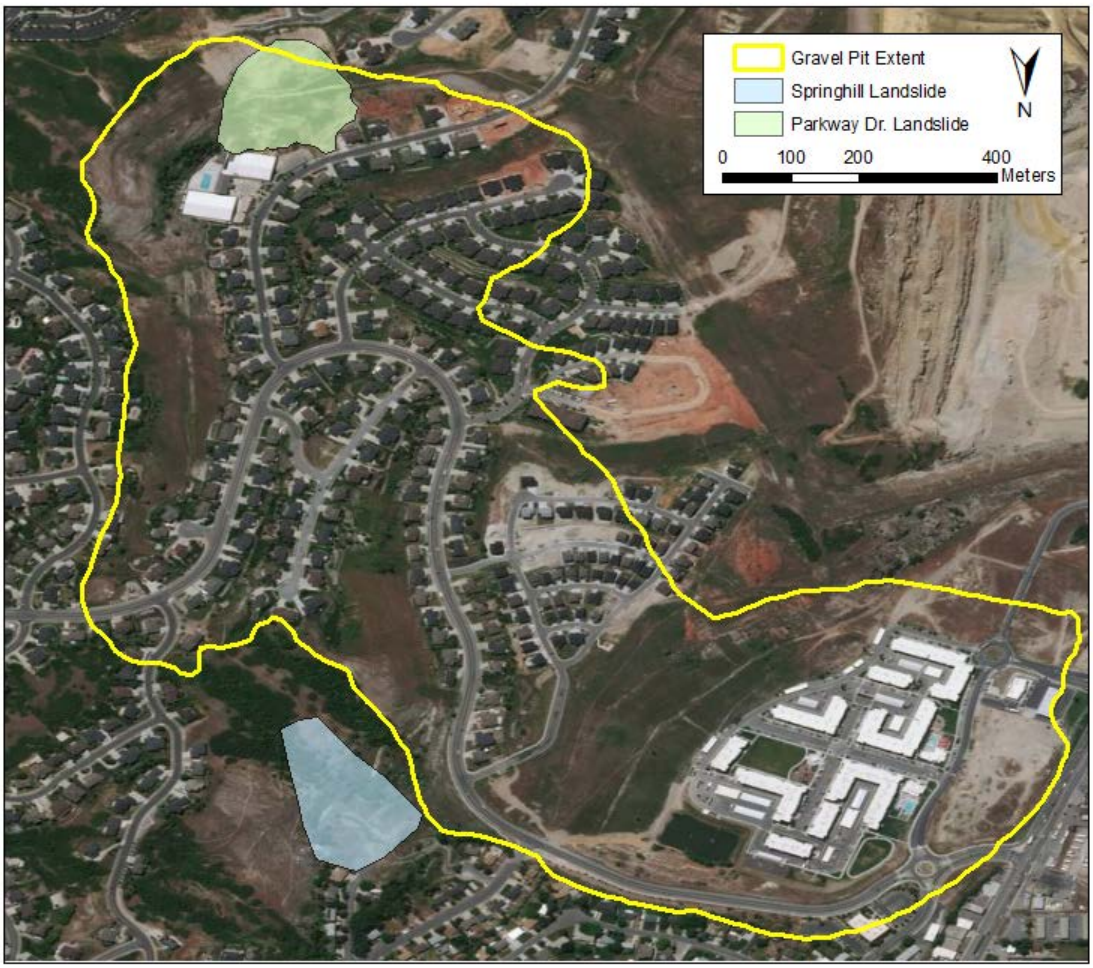


Fig. 10: Full extent of the gravel pit in the 1990s, digitized from aerial photography. The Parkway Drive landslide is located mostly within the gravel pit boundaries, but the Springhill landslide is outside of the boundaries.

move and the stresses on a body begin to overwhelm the strength, tension will create cracks along the surface of that mass. Immediately after the slide occurred, the identified cracks are mainly remnants of mass movement and soils that have not had a chance to reconsolidate.

The aerial photography confirmed that most of the construction (both roadways and homes) surrounding the hillslope occurred from 2004 to 2013 (Figure 11). This construction may have destabilized the slope by cutting material away from the toe as well as adding mass to the top. The increase in ground cracks during those years attest to the decreased stability.

Digital Elevation Models

Digital elevation models were created from a 2013 LiDAR point cloud data set and from a 2015 Structure from Motion point cloud data set from a drone flight. Elevation and slope rasters were created and differenced in ArcMap.

Elevation

Differencing the pre-and post- slide DEMS suggest that the elevation change after the slide differs greatly between the head and the toe of the slide. The head of the slide decreased in elevation as the material moved down slope. Based on the zonal statistics the elevation decreased an average of 7 meters across 6617 m^2 (Figure 12 and 13). That is a volume decrease of approximately 46,000 m^3. The toe of the slide increased in elevation an average of 4 m across an area of 12,710 m^2. That is a volume increase of approximately 51,000 m^3. The total volume of displacement in the slide is 97,000 m^3. The head scarp of

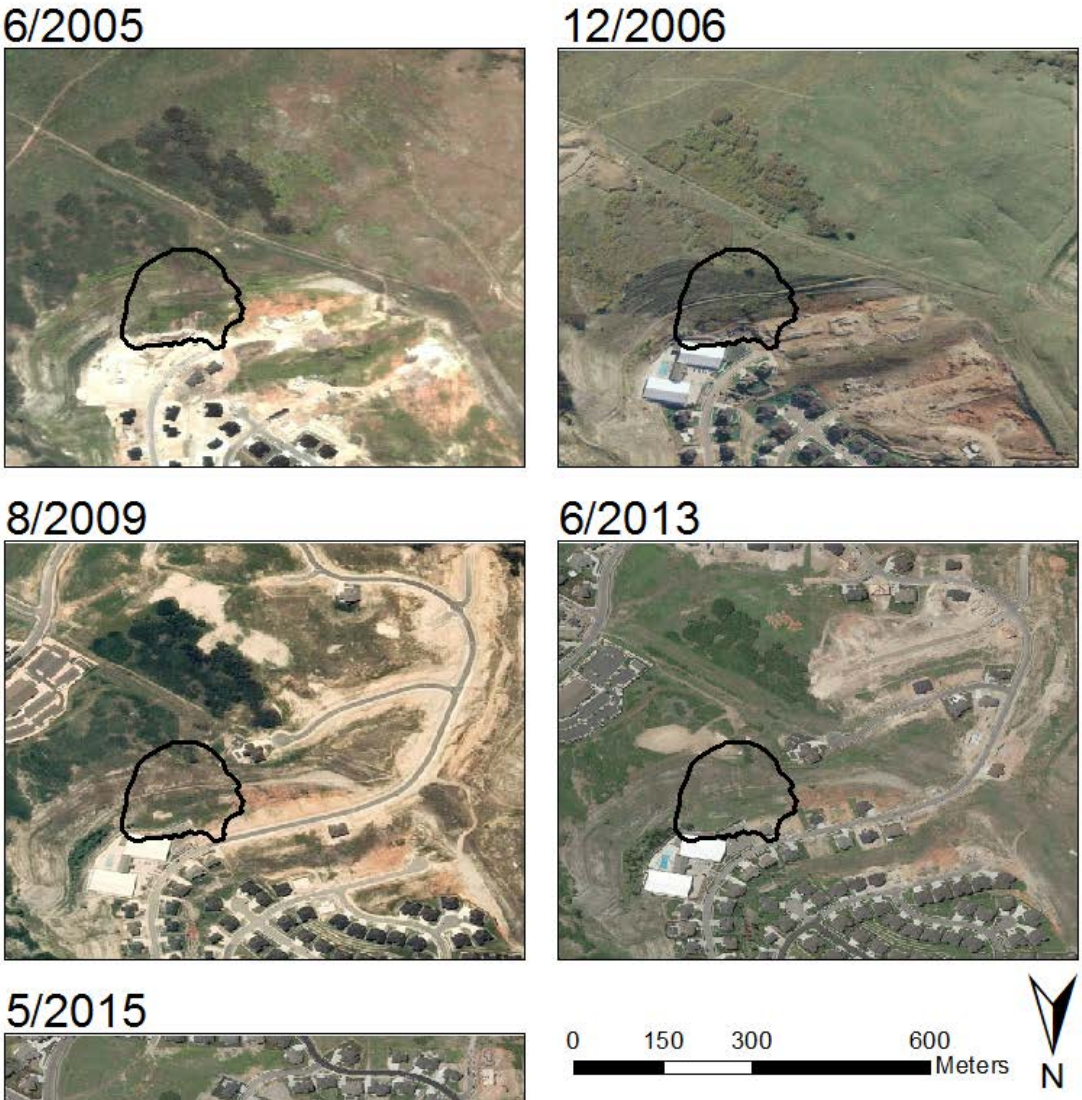
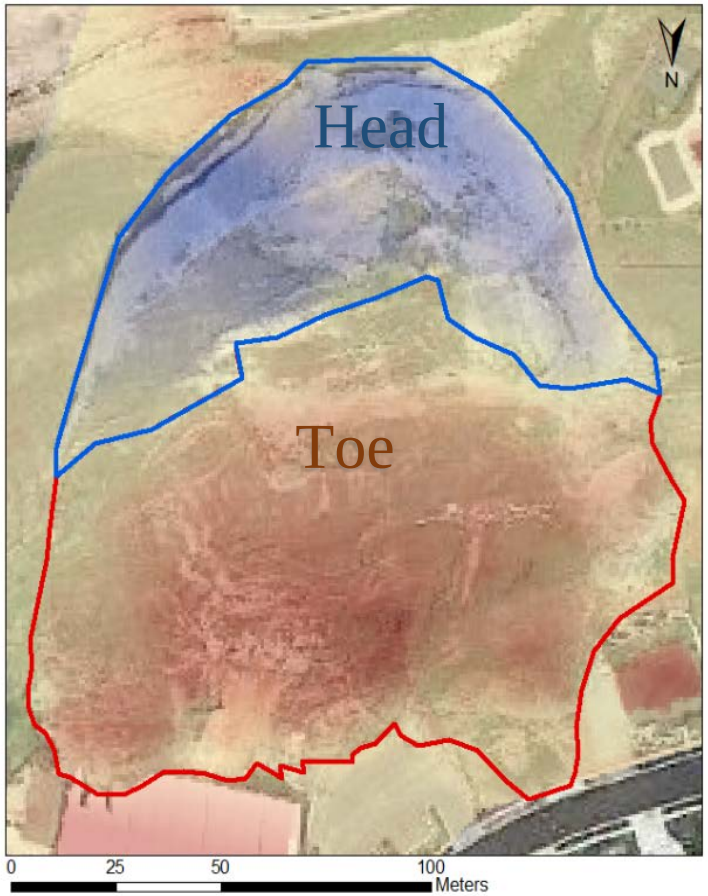


Fig. 11: Modification above the hillslope leading up to the slide. The initial slide extent is outlined in black. By 2009 a church has been constructed above the slope, and by 2015 the neighborhood was constructed. This prevents infiltration and focuses water flow to the slide area.



Head					
Input		Min	Max	Mean	STD
Elevation	Pre	1531 m	1563 m	1550 m	8
	Post	1532 m	1563 m	1543 m	6
	Difference	-14 m	2 m	-7 m	3
Slope	Pre	0°	44°	23°	6
	Post	0°	75°	26°	15
	Difference	-37°	2°	-7°	18
Curvature	Pre	-248	272	0	35
	Post	-936	1020	-6	74
	Difference	-936	1032	-6	82

Toe					
Input		Min	Max	Mean	STD
Elevation	Pre	1499 m	1546 m	1518 m	12
	Post	1500 m	1547 m	1522 m	11
	Difference	-2 m	13 m	4 m	3
Slope	Pre	0°	73°	23°	11
	Post	0°	67°	23°	11
	Difference	-44°	57°	0°	15
Curvature	Pre	-1376	1316	-1	57
	Post	-583	390	0	34
	Difference	-1307	1363	1	65

Fig. 12: The map shows the zones used for the calculations shown in the tables. Blue shading represents elevation lost on the slide and red represents elevation gained.

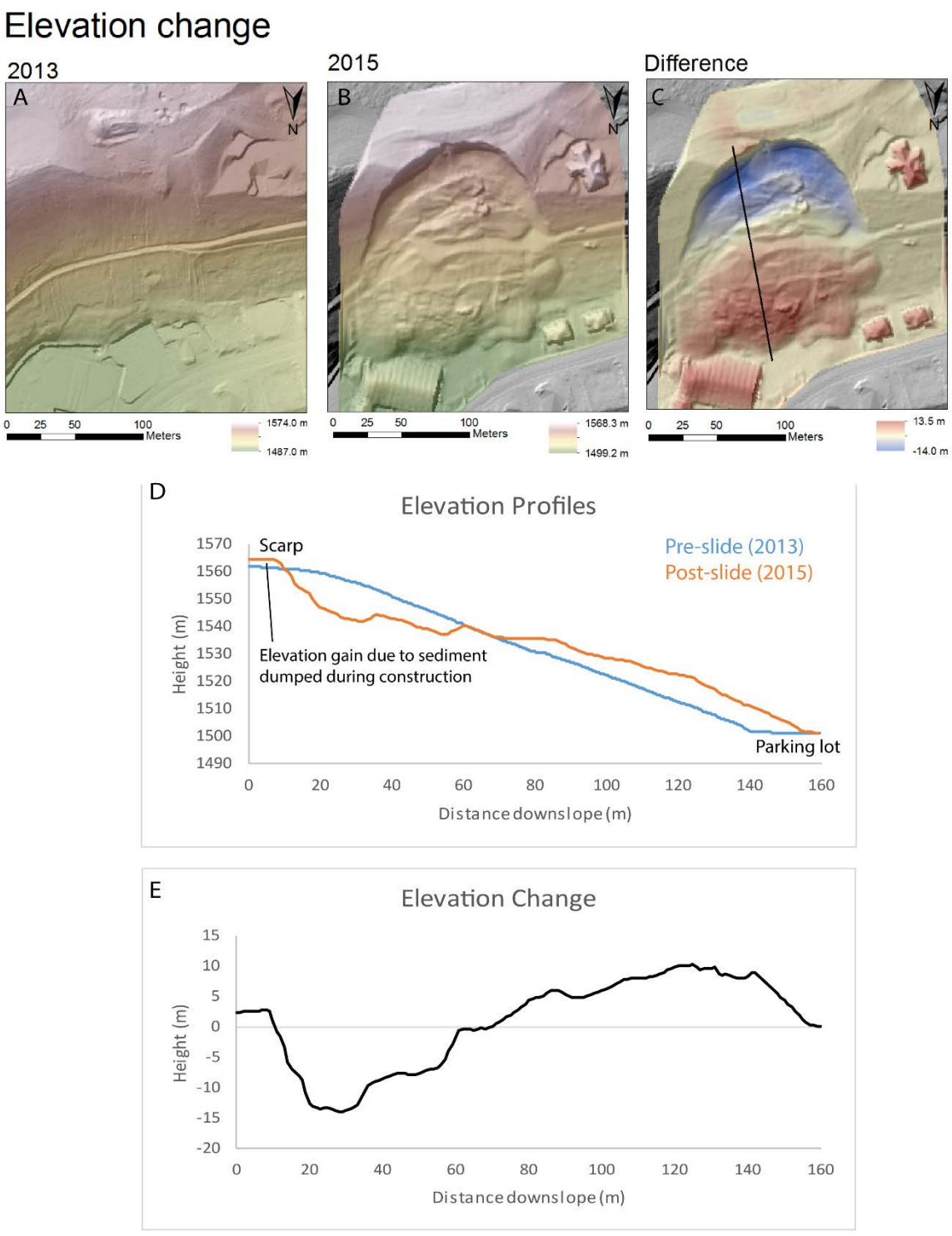


Fig. 13: A & B) Raster outputs of elevation data from DEMs. C) Difference raster from 2013 to 2015. D) Elevation profiles before and after the slide based on transect shown in C. E) Profile of the change in elevation from the differenced raster and the transect.

the slide was 14 meters high, and the greatest increase of elevation at the base of the slide was 13 m where the ground material flowed into the parking lot of the tennis club (Figure 13).

Slope

The slope rasters show a near linear slope before the slide and more varied slope across the slide afterwards (Figure 14). Before the slide, the the highest slope in the DEM was along the hillside behind the Eaglepoint Swim and Tennis Club to the East of the slide location where the hillslope had been cut back and terraced. The average hillside slope of the affected area before the landslide was 24°, which is below the angle of repose for undisturbed gravels (30-35°). Note however, image analysis and field observations indicate that the slope was dominantly underlain by exposed Norwood Tuff. After the slide the head scarp increased locally to an angle of 75°, but the slide overall decreased in slope by an average of 4°. The northeastern side of the toe increased to over 30°, beyond the angle of repose, consistent with subsequent reactivation in the toe of the landslide.

DISCUSSION: Analysis of the pre- and post-landslide DEMs indicate that the greatest changes in the landscape occurred at the headscarp of the slide where the slope initially failed, and mass began moving down slope. However significant changes also occurred at the toe of the slope. The amount of mass moved away from the head of the slope is slightly less than the mass gained at the toe due to dilation within the material as it flowed downslope. This is evidence for a slump with little to no debris flow associated with the mass movement, which is consistent with observations during the slide event.

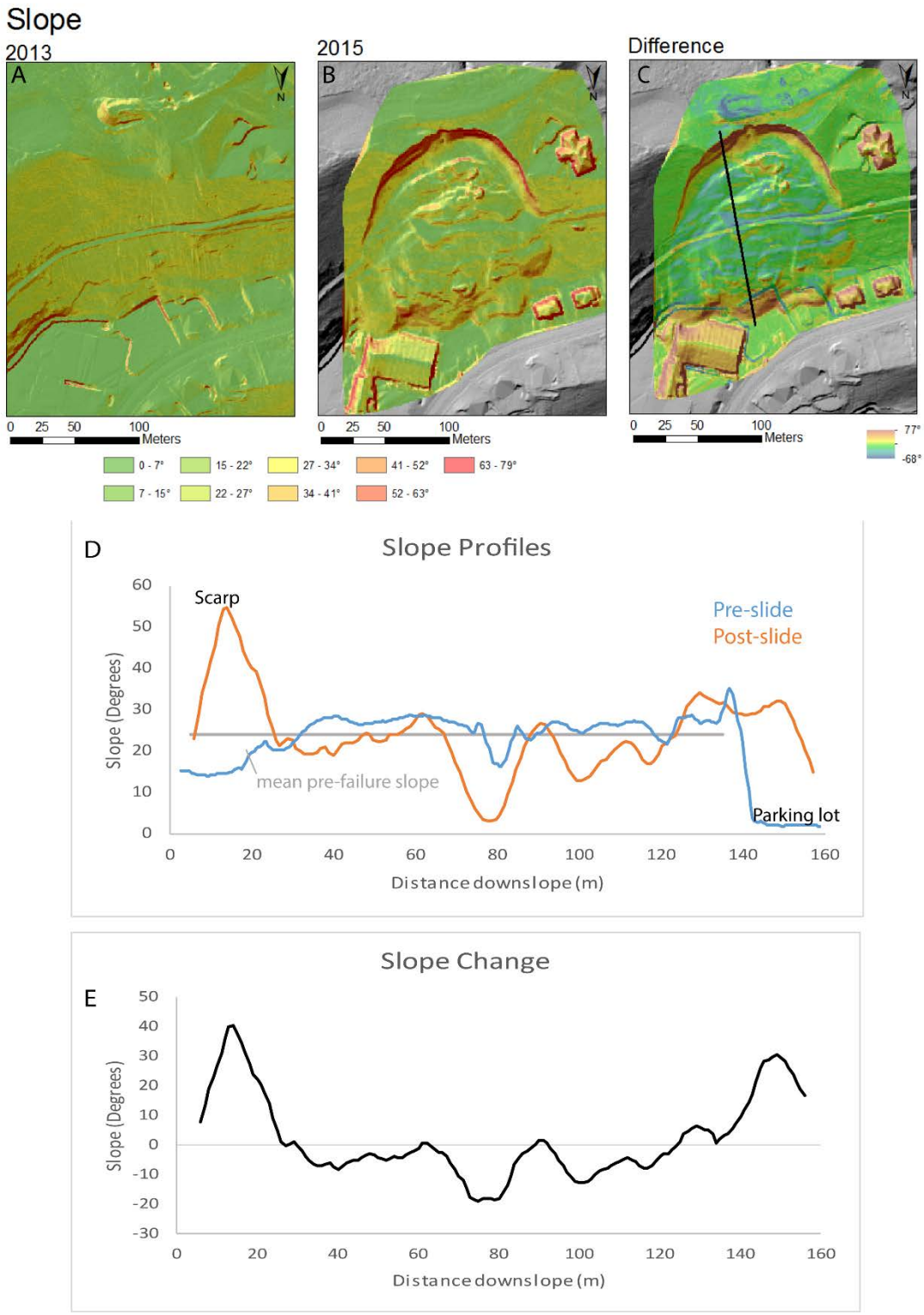


Fig. 14: A & B) Raster outputs of slope data from DEMs. C) Difference raster from 2013 to 2015. D) Slope profiles before and after the slide based on transect shown in C. E) Profile of the change in slope from the differenced raster and the transect.

Before the slide, the slope was graded to an angle of 23°, but slope stability is based on more than the angle alone. The factor of safety equation informs us that an increase in pore water can reduce the friction in the ground and cause slope failure at lower gradients. Continuing with this thought process, the slope east of the slide area, behind the tennis and swim club, is at a steeper gradient than the area of the slide, but it did not fail. However, note that the slope behind the Tennis and Swim club has been terraced near the base, and drained by piping installed by the owner of the club. If the steeper slope remained stable while the lower slope failed, it seems that terracing and draining the groundwater was a successful mitigation effort.

While the body of the slide remained at a generally stable angle of 26° after the event, sections of the toe were steepened beyond the angle of repose (~35°). The oversteepened part of the slope is likely to fail again. Indeed, since 2015 it was documented by the Utah Geological survey that these areas have reactivated as a slow creep and currently threaten both the tennis club and the homes at the base of the slope. The results of these analyses suggest that the slope may have been relatively stable, and an external trigger was responsible for the sudden slope failure.

Construction of roads, neighborhoods, and a church above the slope may have overburdened the top of the slope after it was originally graded. Active construction can be seen in the 2006, 2009, 2013, and 2014 images of Figure 6. Construction of the parking lot below the slope cut into the toe of the slide. Based on the profiles created, there was a slight elevation gain above the headscarp of the slide between 2013 and 2014. Observations from

a photo taken shortly after the slide indicate that excavated sediment was dumped at the top of the hillside (Fig. 15). This is evidence for human alteration that created an unstable hillslope.

Geochemical and Grain-Size Analysis

The locations of the four samples of Norwood Tuff, as well as the contact between the leached and unleached portions of the Norwood Tuff are shown in figure 16, and images of each sample site are shown in Figure 17. Sample PWD050318-1 was collected from a lithified bed of light reddish brown (2.5YR 7/4) volcanoclastic sandstone that contained quartz veins. The sample was quite hard and resistant to attempts to collect it using a sledgehammer. Adjacent sample PWD050318-2 was collected from weathered red (2.5YR 5/6) tuffaceous sediment. This material was wet and soft. Sample PWD050318-3 was collected from a white (N8.5), block of colluvial tuff, consisting mainly of an ash layer. The block this sample was taken from was dislodged and slid down slope to the toe of the slide. Sample PWD050318-4 was collected from the Norwood Tuff material that makes up the majority of the hillslope. It is leached, light greenish grey (GLEY2 8/10Y) fine grained sediment. This sample was found to be composed of 9.5% clay (Fig. 18). The average grain size of the sample is medium to coarse silt, making this sample much finer grained than the other three samples (Fig. 19).

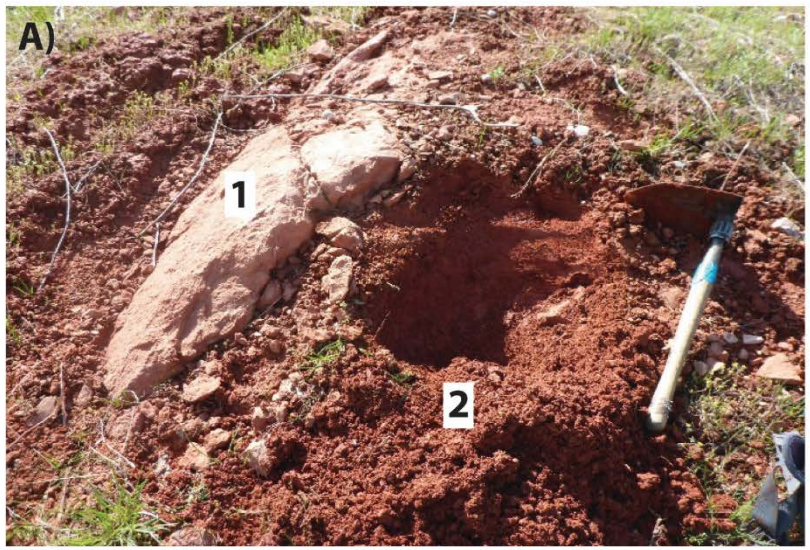
The weathered grey clay material, sample PWD050318-4, shows an enrichment in a few elements compared to the unleached (red) samples 1 and 2. ICPMS analyses indicates that chromium, cobalt, manganese, rubidium, strontium, thulium, lutetium, and thorium were enriched. It is mainly depleted in arsenic (Table 3, and Figure 20). Not every element was



Figure 15: Photo from a few days after the landslide, provided by UGS. Locations of identified anthropogenic fill are outlined in black.



Fig. 16: Sample locations and Piezometer locations. The slide is outlined in white. The black line shows the contact between the red and white sections of the Norwood Tuff. The solid line is GPS measured, the dashed sections extend the contact based on field work and aerial photography



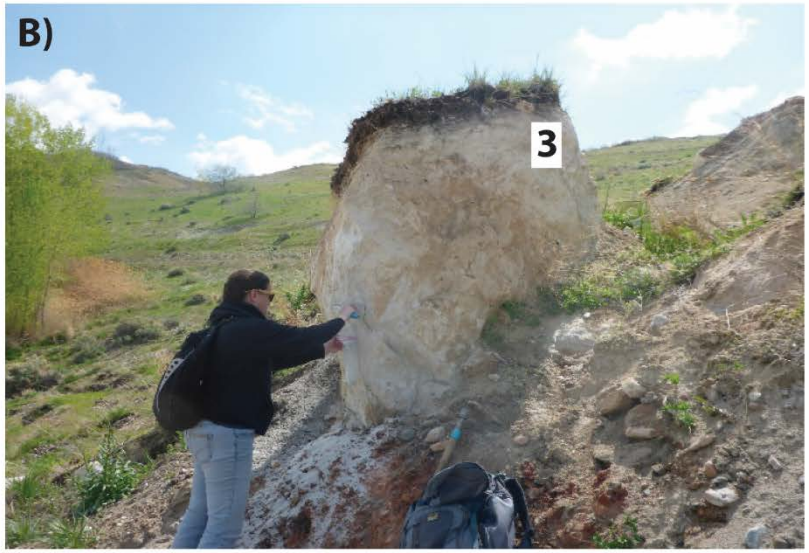




Figure 17: Field photos of the four samples analyzed. The numbers on the photos correspond to the last digit of the sample number.

A) PWD050318-1: resistant red tuffaceous sandstone with quartz veins. PWD050318-2: red sediment weathered from sample one.

B) PWD050318-3: White colluvial ash layer.

C) PWD050318-4: weathered and altered white tuffaceous sediment

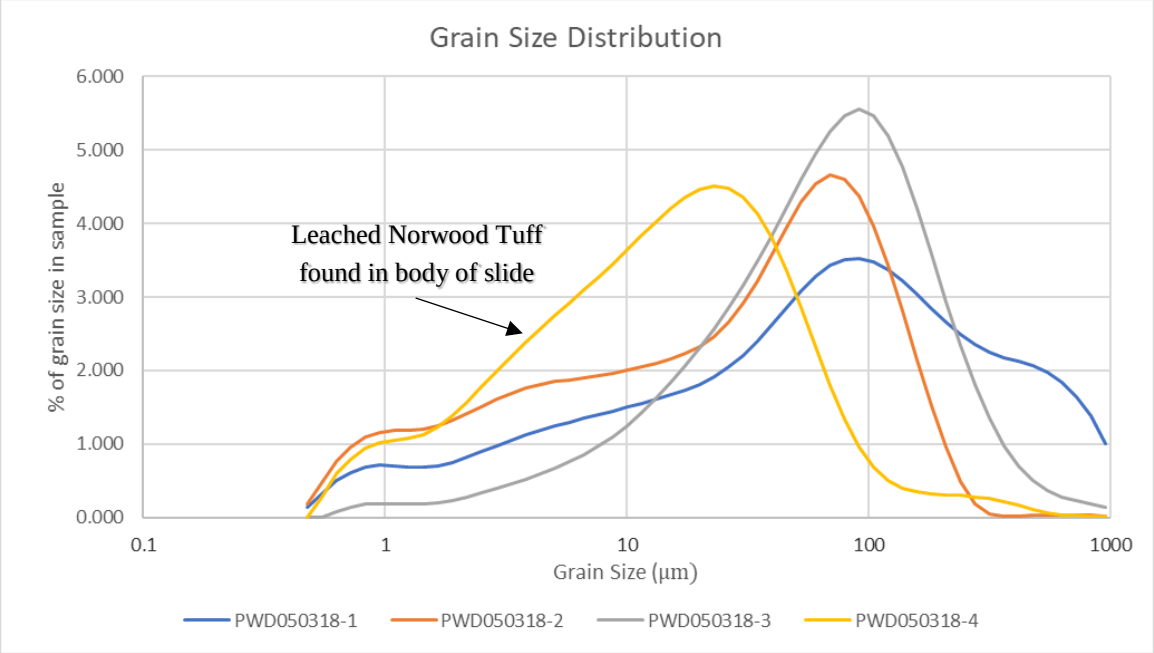


Figure 18: Grain size distributions for each sample

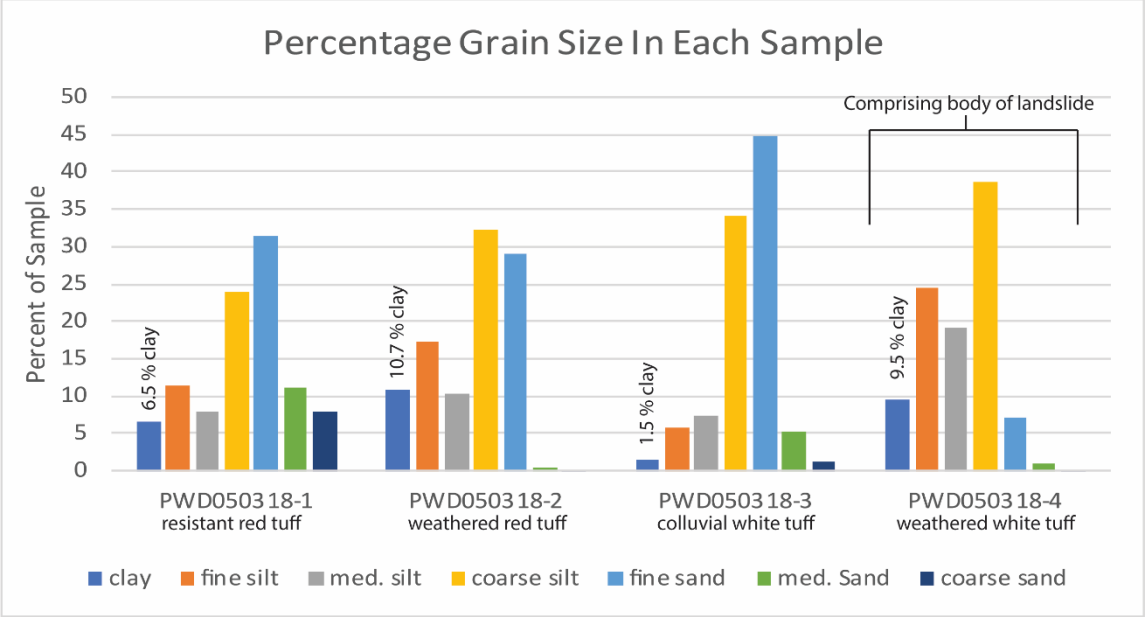
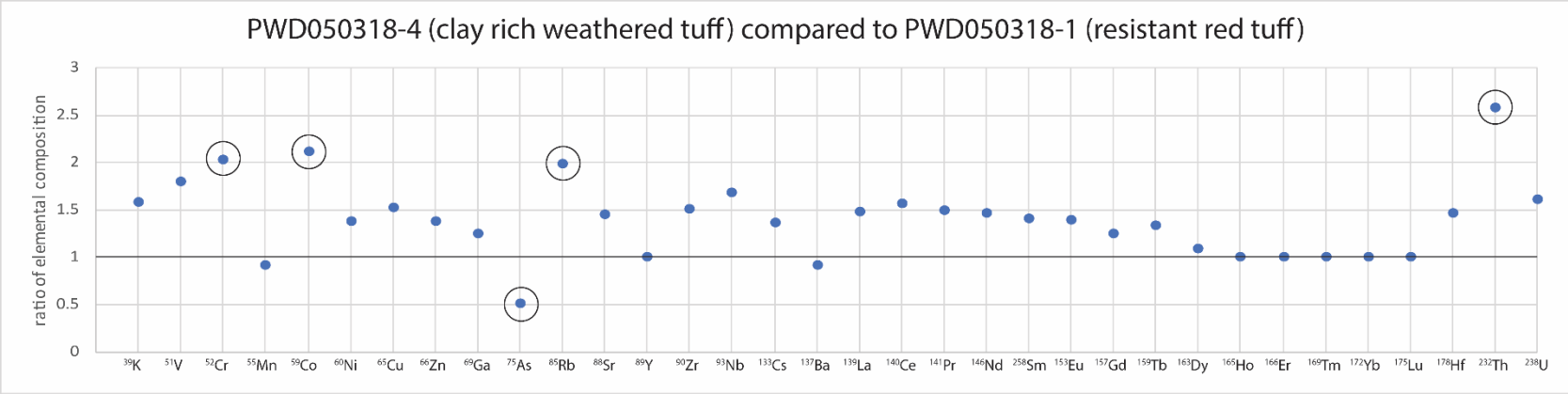


Figure 19: Percentage of each grain size classification in each sample.

Table 3: ICPMS Results in ppm

	PWD-1 1:10	STD	PWD-2 1:10	STD	PWD-3 1:10	STD	PWD-4 1:10	STD	BHVO-1 1:10 USU values	BHVO-1 GEOREM values	accuracy ratio
^{39}K	7856.8	47.7	15082.2	79.2	37222.6	322.1	12410.9	12.5	3955.3	4363	1.1
^{51}V	23.4	0.4	41.1	0.3	0.6	0.1	42	0.5	307.5	313.8	1
^{52}Cr	21.6	0.4	42.5	0.4	6.4	0.1	43.9	0.3	268.3	287.6	1.1
^{55}Mn	268	4.7	69.2	1	261.9	1	246.7	0.8	1271.6	1308	1
^{59}Co	3.2	0.2	4.8	0.1	0.6	0	6.8	0.2	41.7	44.9	1.1
^{60}Ni	10.6	0.3	15.3	0.4	1.8	0	14.6	0.3	110.1	120	1.1
^{65}Cu	10.2	0.1	20.8	0.4	5.5	0.2	15.6	0.3	140.9	137.2	1
^{66}Zn	41.8	0.4	47.3	0.6	73.4	1.3	57.9	0.6	104.7	105.1	1
^{69}Ga	18.6	0.3	26	0.3	30.1	0.6	23.3	0.2	25.1	21.3	0.8
^{75}As	5.1	0	7.8	0.1	2.6	0.1	2.6	0.1	0.7	0.6	0.8
^{85}Rb	37	0.5	65.4	0.7	189.2	0.9	73.4	0.7	8.8	9.5	1.1
^{88}Sr	101.3	0.4	53.2	1	58.6	1.5	147.3	1.1	411.6	399.2	1
^{89}Y	11.8	0	8.1	0.1	66.6	0.5	11.8	0.5	23	26.2	1.1
^{90}Zr	55.9	0.6	82.9	5.8	194.7	1.4	84.1	4.9	154.6	174.6	1.1
^{93}Nb	2.9	0.4	5.1	0.1	54.7	2.4	4.9	0.1	14.6	18.5	1.3
^{133}Cs	4.4	0.1	7.2	0	3.4	0	6	0			
^{137}Ba	383.6	5.2	454	4.9	222.9	2.7	350.7	2.9	147.4	134.4	0.9
^{139}La	14.2	0.2	14.1	0.1	85.8	1.2	21.1	0.1	15.9	15.4	1
^{140}Ce	24.6	1.1	28.4	2.7	161	2.7	38.5	0.3	39.8	38.1	1
^{141}Pr	3	0	3.5	0.1	17.6	0.1	4.5	0.1	5.5	5.4	1
^{146}Nd	11.5	0.1	13.8	0.6	64.2	1.1	16.8	0.3	26	24.8	1
^{147}Sm	2.2	0.1	2.7	0.1	12.9	0.3	3.1	0.1	6.5	6.2	0.9
^{153}Eu	0.5	0	0.6	0	0.5	0	0.7	0	2.2	2.1	0.9
^{157}Gd	2.4	0.1	2.4	0.1	13.6	0.2	3	0.1	6.9	6.3	0.9
^{159}Tb	0.3	0	0.3	0	2.1	0	0.4	0	1	0.9	0.9
^{163}Dy	2.1	0	1.8	0.1	13.3	0.2	2.3	0.1	5.9	5.3	0.9
^{165}Ho	0.4	0	0.3	0	2.7	0	0.4	0	1.1	1	0.9
^{166}Er	1.3	0	1	0	7.9	0.1	1.3	0	2.9	2.5	0.9
^{169}Tm	0.2	0	0.1	0	1.1	0	0.2	0	0.4	0.3	0.9
^{172}Yb	1.4	0	1	0	7.4	0.1	1.4	0	2.3	2	0.9
^{175}Lu	0.2	0	0.1	0	1.1	0	0.2	0	0.3	0.3	0.9
^{178}Hf	1.9	0	2.6	0	8.3	0.1	2.8	0	5.1	4.4	0.9
^{232}Th	3.6	0	5.7	0.1	29.3	0.1	9.3	0	1.3	1.2	0.9
^{238}U	1.3	0	1.9	0.1	7.1	0.1	2.1	0	0.5	0.4	0.8



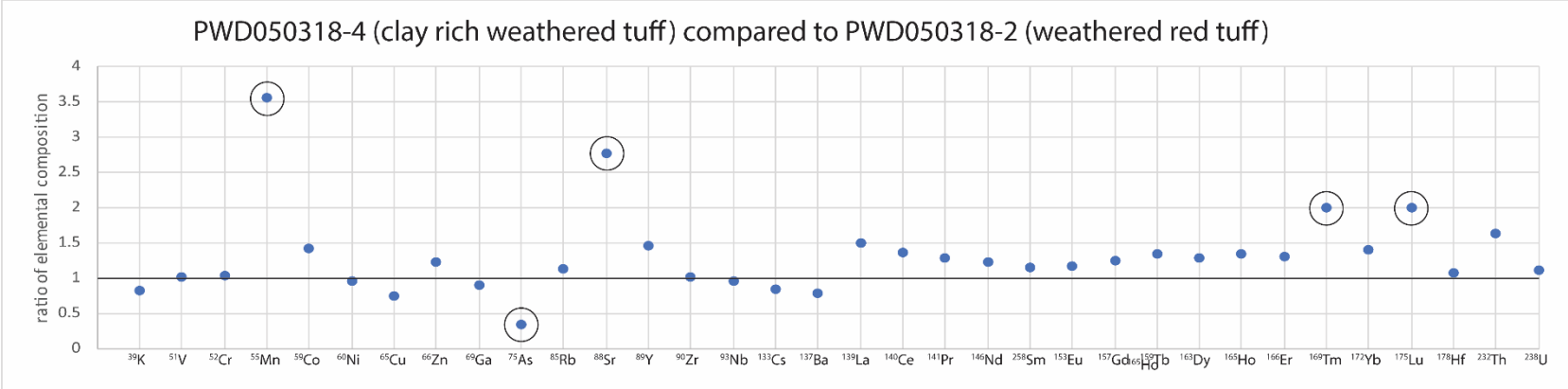
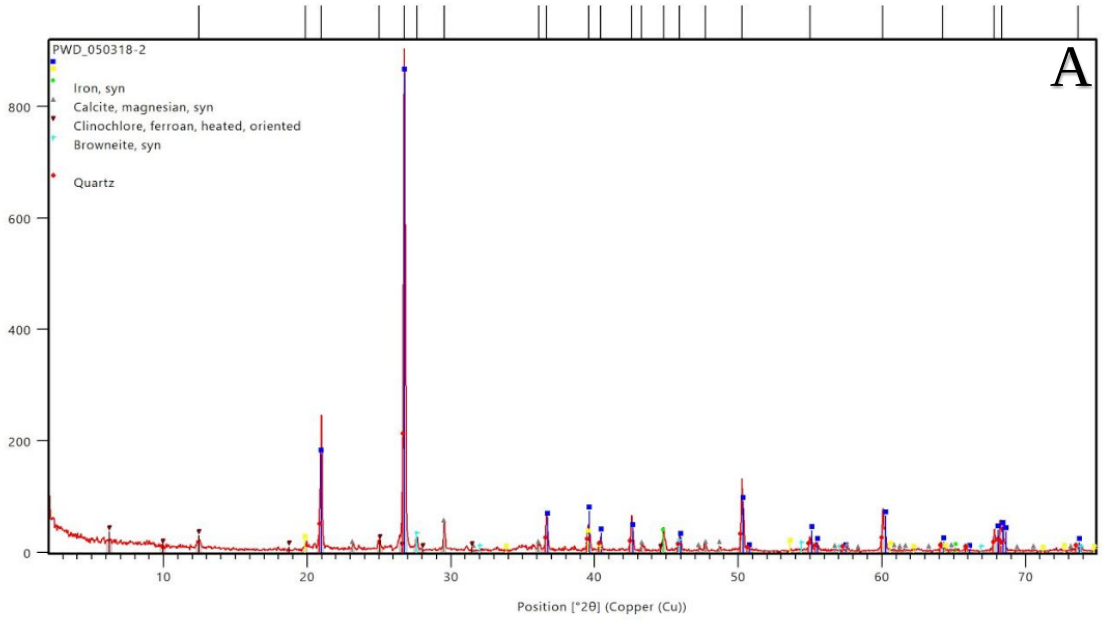


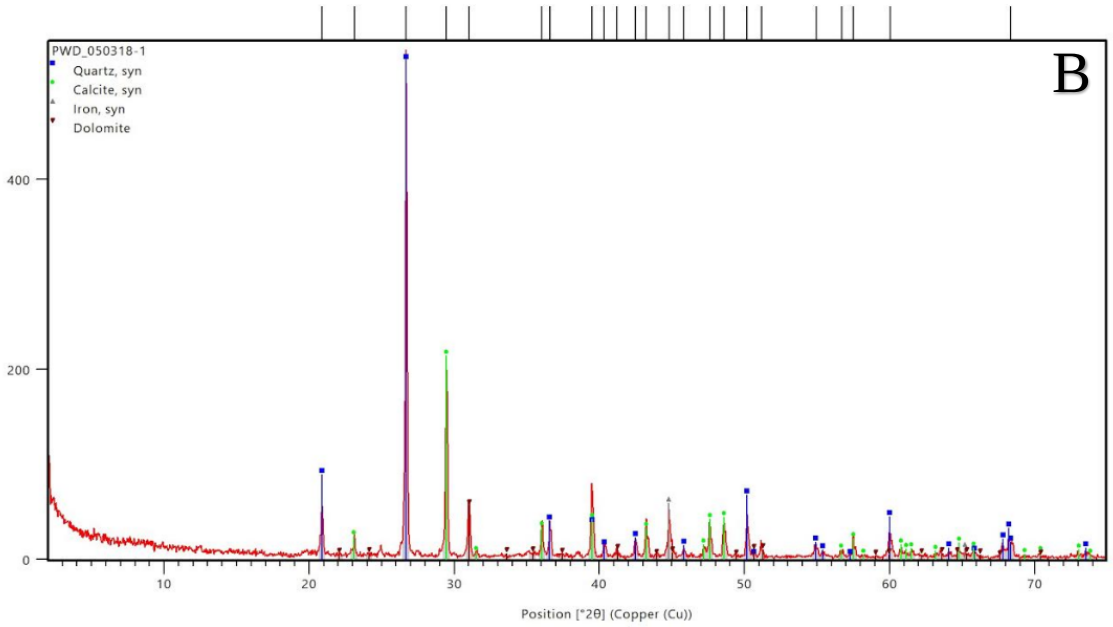
Figure 20: Enrichment values of elements in sample four compared to samples one and two. Top shows comparison to sample 1, bottom is comparison to sample 2. Points above the value of 1 are enriched in the sample, elements below 1 are depleted. Significant enrichment or depletion occurring in each comparison are circled.

analyzed in this run, but it is assumed that this material is also leached of iron and silica. These assumptions are corroborated by the XRD results. Samples 1 and 2 contain a high concentration of quartz and iron bearing minerals like ferroan clinochlore, but sample 4 has more magnesian calcite and montmorillonite clay (Fig. 21).

DISCUSSION: The results from sample analysis demonstrate that the weathered and leached material, sample 4, has the finest grain size, and the most clay. This material is also coincident with spring outlets along the hillslope. This suggests that not only is this material a less competent unit, it also has a high pore water content. The XRD data show that it contains the clay mineral montmorillonite. This is a smectite clay mineral that expands when it becomes saturated with water (Mikhail, Guindy, & Hanafi, 1978). This material comprised the main body of the landslide, suggesting that the expansion of the clays when they were saturated disrupted the cohesion of the soil and bedrock and caused the slide to occur. The western boundary of the slide occurred at the contact between this clay rich white volcanoclastic sediment (sample 4) and the more resistant red tuff (sample 1).

While not immediately related to the geotechnical aspects of the Norwood Tuff underlying the landslide, it is interesting to note that the less competent and clay-rich white units of the Norwood Tuff is depleted in arsenic compared to the red units. The white units are associated with springs and greater groundwater flow it is possible that the arsenic was leached into the groundwater. It might be important to analyze the spring water for arsenic content.


A
PWD_050318-2
Iron, syn
Calcite, magnesian, syn
Clinochlore, ferroan, heated, oriented
Browneite, syn
Quartz
800
600
400
200
0
10
20
30
40
50
60
70
Position [°2θ] (Copper (Cu))


B
PWD_050318-1
Quartz, syn
Calcite, syn
Iron, syn
Dolomite
400
200
0
10
20
30
40
50
60
70
Position [°2θ] (Copper (Cu))

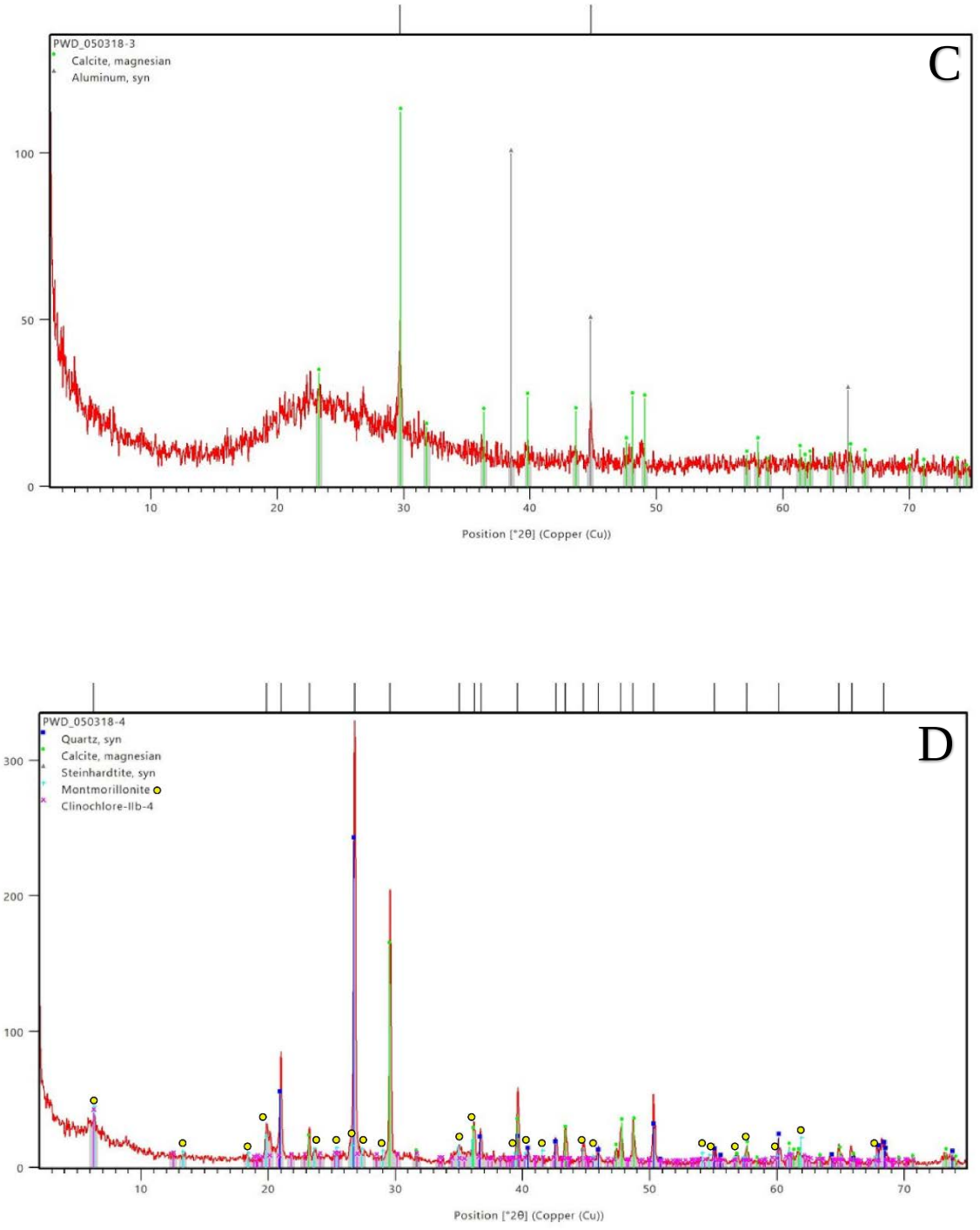


Figure 21: Profile results from XRD analyses. Samples 1, 2, 3, and 4 are shown in A, B, C, and D respectively. Notably sample four has many peaks that include the clay mineral, montmorillonite, shown with the yellow circles.

Field Observations and Survey Results

The results from the GPS surveying performed by the UGS after this slide were provided by Ben Erickson (Fig. 22). The major movements since the slide event have been located in the northeast and northwest sections of the toe. There has been about 40 inches (101.6 cm) of downslope movement on the western side of the slide and 110 inches (279 cm) to 190 inches (483 cm) of downslope movement in the center of the slide over the 2014 – 2017 interval. It corroborates the aerial photography and DEM analyses that suggested these areas are the most unstable as evidenced by the occurrence of ground cracks and steeper post slide slopes.

The main mitigation efforts on this slope are shown in Figure 23. The head of the slide was regraded back to reduce the overall slope and remove material from the head. Boulders were placed in the section just below the regraded headscarp. Surface drain pipes and shallow canals were also added to the center of the slide to reroute water away from the slide. Another pipe was connected to the two canals to funnel the water directly into the storm drains along the road, but that pipe has since detached so the original placement could not be mapped.

DISCUSSION: The mitigation efforts appear to have varying results. The drain es and canals were designed to route overland flow away from the landslide body. The drains may have been minorly effective in that overland flow was captured, but underground springs and groundwater flow was not halted, so there was not a large reduction in groundwater flow and saturation of the sediments and leached Norwood Tuff under the main body of the slide. Within two years of installation, the pipe leading away from the slide was dislodged and broken. It was unearthed and is now visible (Personal observation, 2017). The UGS has stated that they have never witnessed water flowing out of that end,

suggesting that even when the pipe connected, no water flowed out of it. The placement of boulders on the landslide appears to be counter-intuitive. While it may increase internal friction and roughness of the surface sediments, it places a

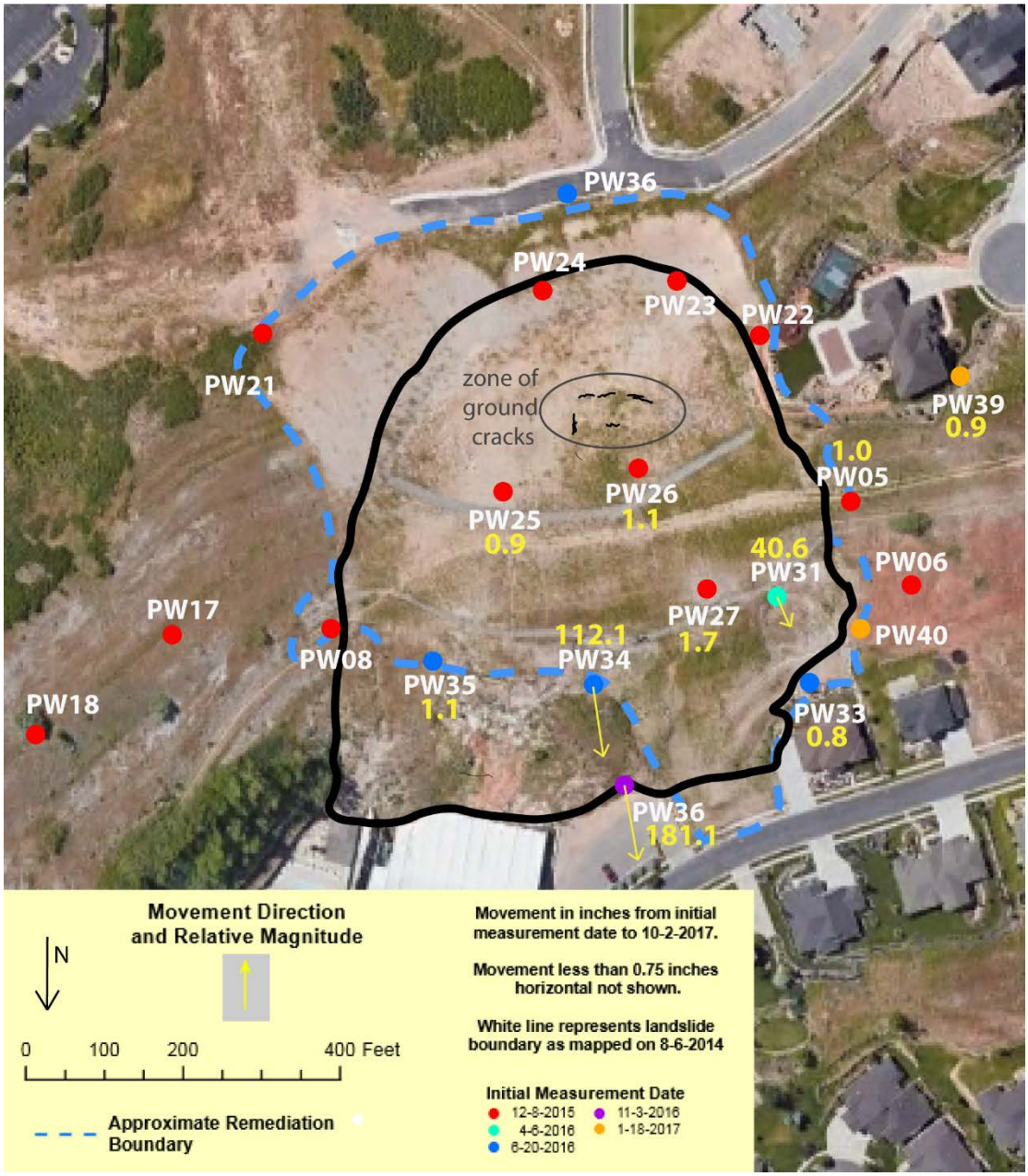


Fig. 22: GPS data from the Utah Geological Survey. Main areas of movement are the northeast and north west. Figure modified from one made by UGS.

larger burden on the slope by adding mass to the head of the slide. The regrading of the slope was likely the most effective method of mitigation. There have been no further tension cracks or movement along the re-graded area. The problem is that they only regraded the top half of the slide, leaving the toe over steepened and prone to future movement.

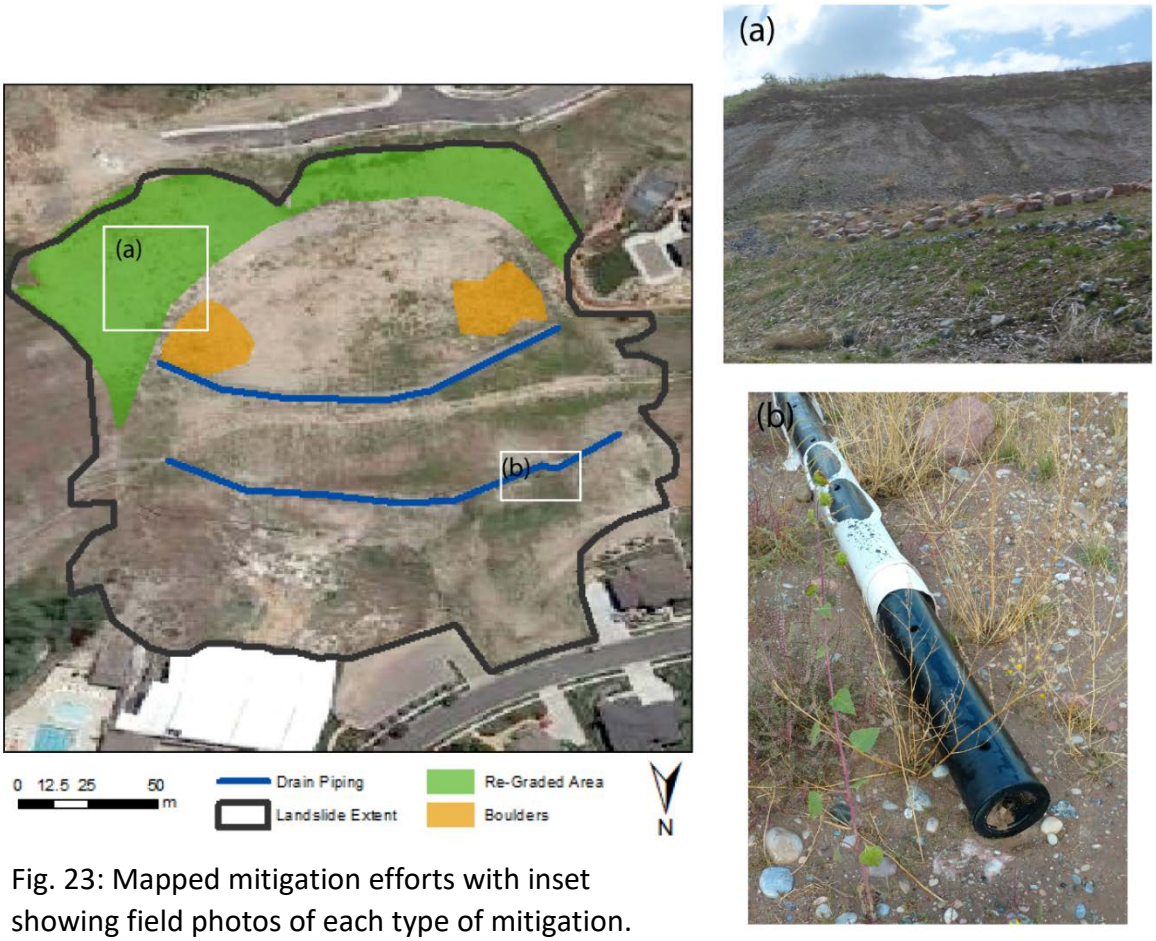


Fig. 23: Mapped mitigation efforts with inset showing field photos of each type of mitigation.

Precipitation

A 3rd hypothesis about the trigger of this slide is that 2014 was an unusually wet year and that the excess precipitation raised the water table and caused the landslide. After compiling the monthly precipitation data from the NOAA station at City Creek, this hypothesis is proven incorrect. Figure 24 shows a monthly compilation of precipitation data from 2000 until the end of 2016. These data show that 2014, in fact, was a dry year for North Salt Lake, with 2013 being a wet year. However, there were two significant rain storms in the week leading up to the slope failure. On July 29th (six days before the failure) there was a large thunderstorm that produced 16 mm of rain, and an additional 11 mm of rain fell the night before the slide.

DISCUSSION: The results of the analysis of the precipitation data from the City Creek NOAA station showed that the beginning of 2014 was drier than most years. There is a slight correlation between the amount of precipitation in a year and the increase in ground cracks, indicating that precipitation is affecting ground motion along this slope (Fig. 25). Based on the monthly average data, 2014 was a relatively dry year suggesting that the slope failure was not linked to ambient precipitation levels. However, six days before the landslide (July 29th, 2014), there was a significant rainstorm that produced 16 mm of precipitation in 48 hours (Fig. 26). This is more rain than the area normally has in the entire month of July (Fig. 27). There was also a significant thunderstorm the night before the landslide release where the area received 5 mm of rain (a third of the monthly average) in just one hour ("Salt Lake City International, UT History | Weather Underground," 2014).

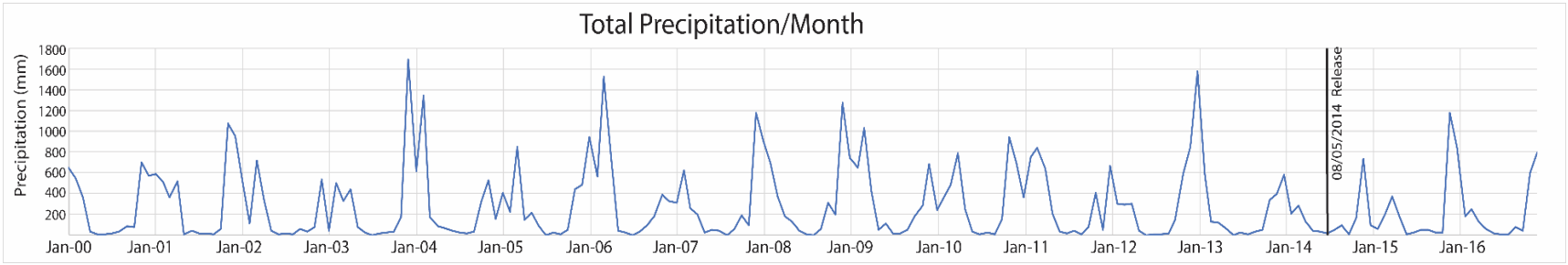


Fig. 24: Monthly accumulation of precipitation. The line is the date of the landslide.

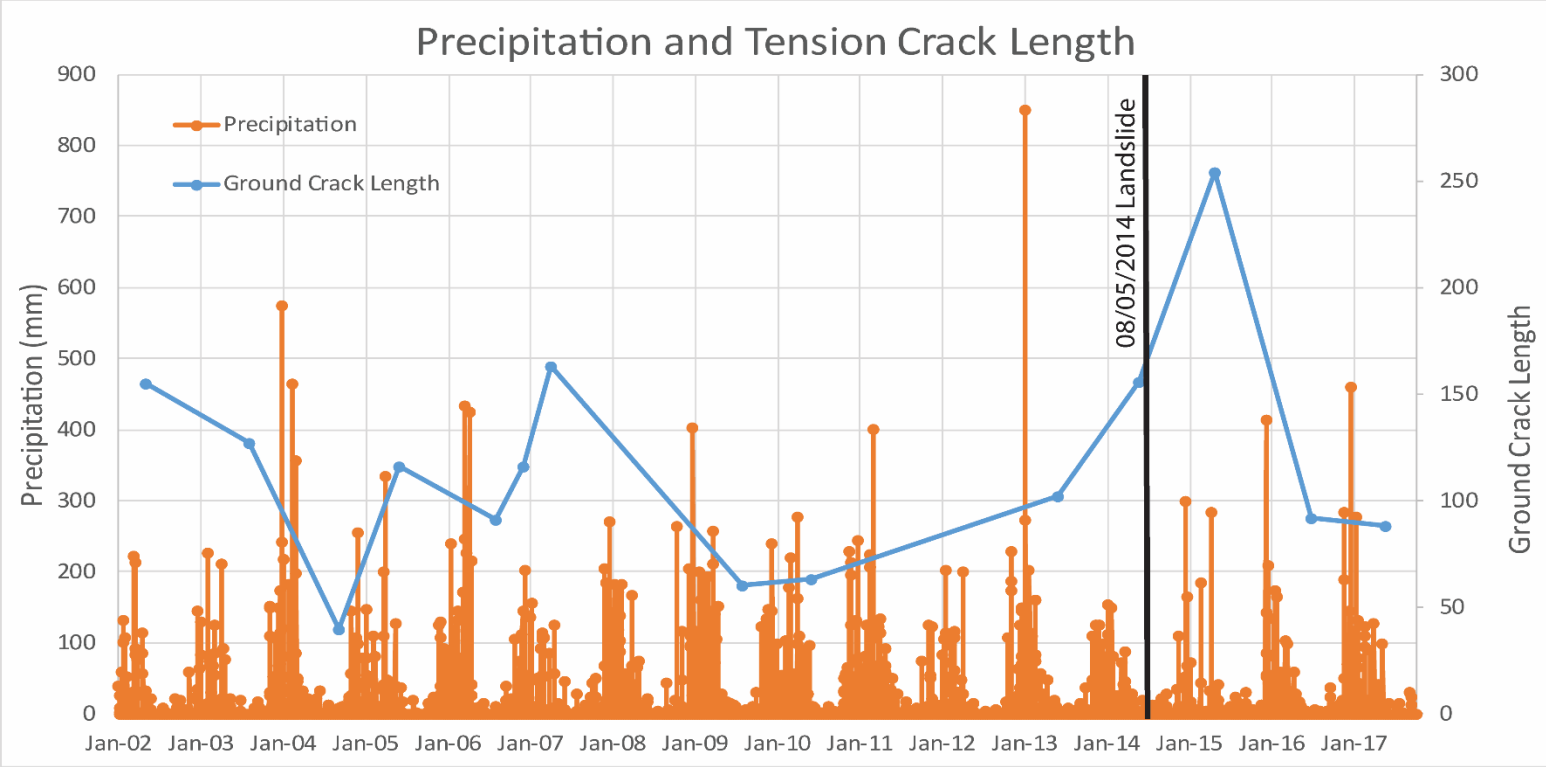


Figure 25: Precipitation plotted monthly compared to ground crack length plotted based on available data. General trends show increasing length of ground cracks following years with higher precipitation. This is especially apparent following 2006 and 2013.

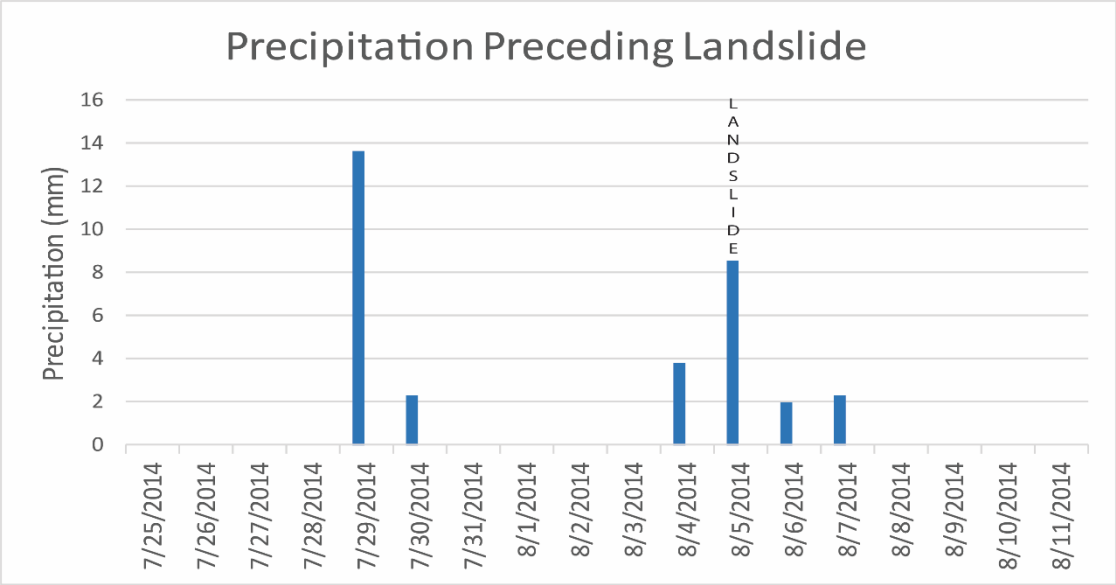


Figure 26: Precipitation leading up to the day of the landslide. The main storm occurred on July 29th.

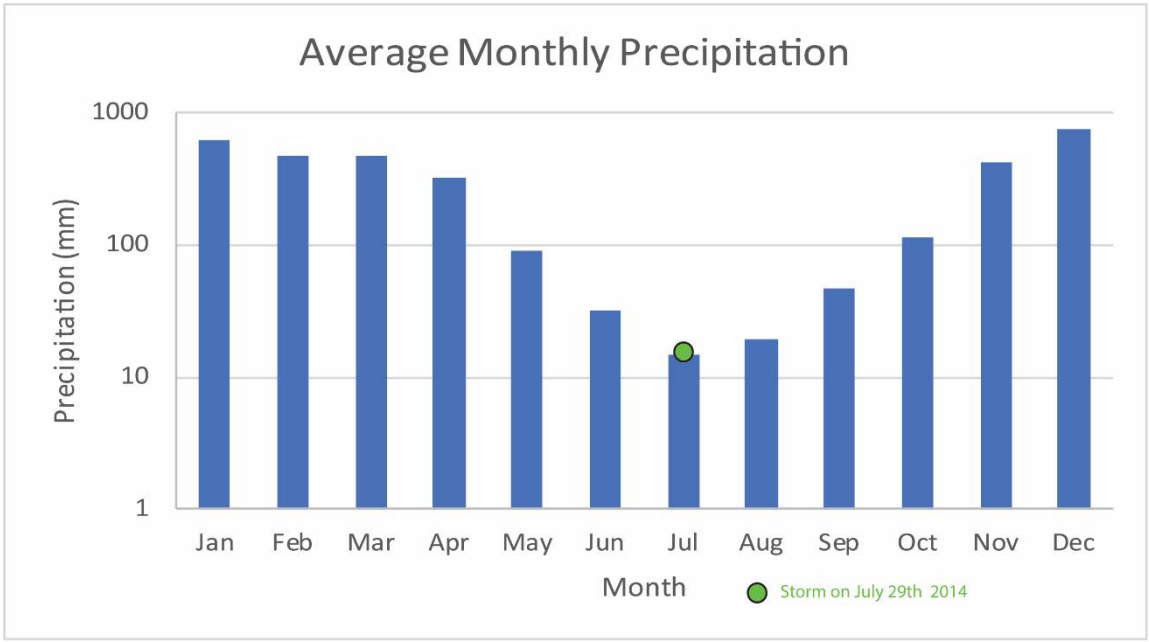


Figure 27: Average precipitation by month for 2000-2016. The green dot represents the precipitation from the storm July 29th 2014, which was just over the average precipitation for July.

The influx of precipitation may have quickly infiltrated the dry ground and created enough of a reduction in friction and buoyancy within the ground mass to cause motion. The differential permeability between the gravels and the clay-rich tuff would locally concentrate water at the contact. This slope drains a large area of the bench above it, so even a slight rainstorm could easily concentrate water at the contact, and saturate the clay-rich tuff unit (Fig. 28). Development of buildings and roads above the hillslope beginning in 2004 increased impervious surfaces which increases runoff and focuses infiltration in the area of the slide. The homeowners living along that bench also irrigate their lawns and/or gardens, adding more water to the system beyond just precipitation events.

Shallow groundwater monitoring wells would be instructive to assess the relationship between precipitation and water content within the area that failed. Piezometers were installed in the landslide body in late 2015 to early 2016 (after the landslide). The locations of these two meters, as well as a third meter down slope from the landslide can be seen in Figure 16. Piezometer PW-1E is located on the eastern side of the slide, about halfway between the headscarp and the toe of the slide. Piezometer PW-2W is located to the west of PW-1E at approximately the same elevation. Monthly averages of groundwater level was compared to the monthly total precipitation for the same time frame (Fig 29). Piezometer PW-2W does not respond as significantly to precipitation event as PW-1E. There were only 12 months of data available for this site, which makes it difficult to determine a groundwater lag time. More data will be needed to make a solid conclusion.



Figure 28: Surface drainage and spring outlets of the Parkway Drive landslide overlain on a google earth image from 2013. The spring outlets indicate underground flow, and the streaks shown in the image indicate overland flow when the hillslope becomes saturated.

Seismology

Seismic data from the University of Utah seismic station were compiled to test the hypothesis that seismic shaking induced hillslope failure. (Fig 30). These data indicate that there were few seismic events leading up to the landslide. The average seismic event leading up to the landslide was approximately a magnitude 1.3.

DISCUSSION: The seismic data analyzed shows that there was not an unusually large number of seismic events, nor were the magnitudes larger than usually seen in this area. It is unlikely that seismic shaking initiated the release of this landslide. If any reduction in friction and therefore stability occurred because of this shaking, then it would have affected this slope in the exact same manner throughout the entire 16 years that were analyzed. The background seismic shake may reduce stability, but it did not affect this event specifically.

CONCLUDING OBSERVATIONS AND COMMENTS

The Parkway Drive landslide moved approximately 97,000 m^3 of material down a 24° graded slope in an urban neighborhood in North Salt Lake, UT (Fig. 31). The hypotheses presented at the start of the research were that failure was caused by, 1) the properties of the underlying sediments and rocks, 2) rainfall events and hydrologic characteristics of the slope, 3) seismic shaking, and/or 4) that it was caused by human modification to the landscape. The leached Norwood Tuff bedrock underlying the slope appears to be weaker than the adjacent red colored and more resistant parts of the Norwood Tuff based on its weathering characteristics and appearance. Moreover, the high clay content of the leached tuff under the landslide is consistent with an unstable slope prone to failure. The high

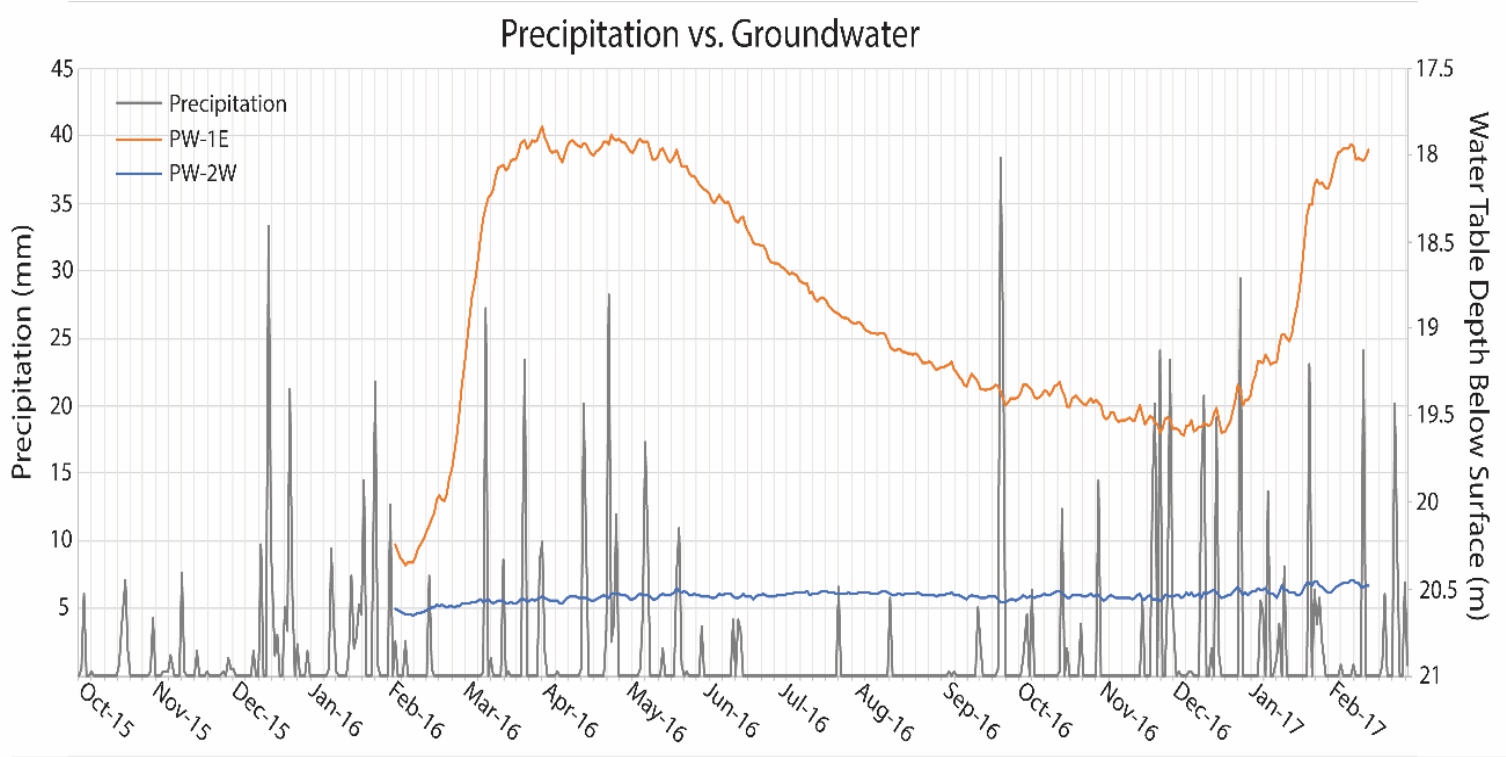


Fig. 29: Groundwater depth compared to precipitation recorded daily. Groundwater on the right axis and precipitation is on the left axis. Each gridline is 5 days.

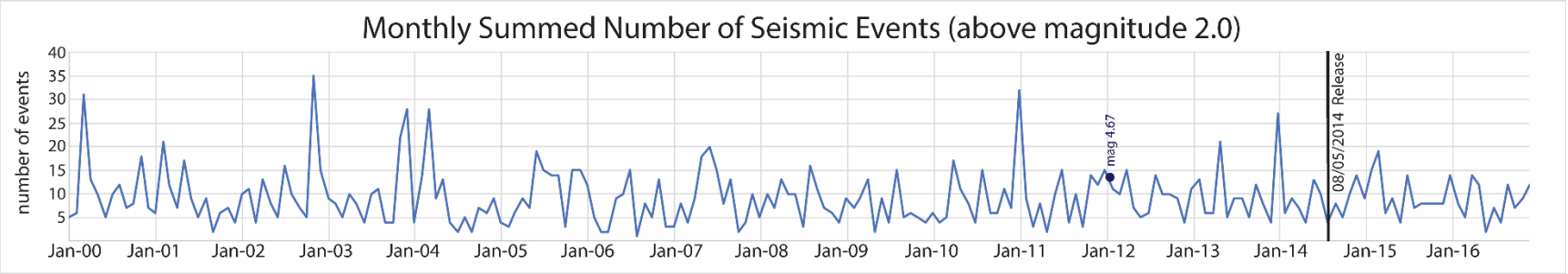


Fig. 30: Number of recorded seismic events over a magnitude of 2.0 per month. The line is the date of the landslide. Two events over magnitude 4 are shown on the graph



Figure 31: Conceptual model of the failure at the Parkway Drive on Aug. 5th, 2014. The head of the slide was overburdened during construction. The failure plane existed primarily within the Norwood Tuff unit.

precipitation events six days and the night before the hillslope failure suggest a causal mechanism, In addition, the development, roadways, and parking lots in the neighborhood above the landslide headscarp likely lead to reduced infiltration capacity and greater runoff and localized points of infiltration. This would have increased the concentration of water in the hillslope prior to failure. Seismic activity does not seem to have been a factor as there were no significant seismic events associated with the landslide. Human modification to the slope such as regrading of the slope after gravel pit operation terminated, and continued construction both above and below the hillside, is likely to have added to the destabilization of the slope.

Results of this study suggest that characteristics of the Quaternary geologic sediments and the bedrock geology underlying the slope, rainfall events and hydrologic characteristics of the slope, and human modification to the landscape all contributed to destabilizing the slope and played a role in the slope failure. Research based on aerial imagery, digital elevation models, geochemistry and grain size analyses, field observations, precipitation monitoring, and seismic monitoring suggest six main contributing factors to the slope failure. They are listed below, in no particular order.

1) The rock unit underlying the slope is a weathered and altered white tuff that has a high clay content. This clay is montmorillonite, a mineral that expands readily when saturated with water. This makes the material underlying the slope weak, and prone to failure.

2) The slope contains both surface and underground conduits for water flow which focus drainage in the slide area. Surface flow is drained from a larger portion of the bench above and at least two springs outlet on the face of the slide. This groundwater flow would

continue to weather the tuff and create a positive feedback loop, saturating the tuff so it expands, reducing the grain to grain friction, and leading to ground movement.

3) The porous Bonneville gravel deposits overlay the less porous Norwood Tuff unit in this area, creating a contact that could act as an impermeable boundary. This may consolidate water at the contact, saturating the area and creating a plane of weakness that could lead to failure.

4) The hillslope was engineered and graded to an angle determined safe for housing development. This angle was based on the characteristics of the Bonneville gravels. An engineered slope is not as stable as a slope that developed naturally and has had time to erode and settle due to compaction. The gravels only make up the thin veneer of sediment above the Norwood Tuff unit. Due to these factors, the area may not have been safe for further development.

5) There was continued human modification to the slope since the area was reclaimed in the early 2000s. The Eaglepoint Tennis Club construction undercut the toe of the slope in multiple areas, particularly during the construction of the parking lot. The construction of a neighborhood on the bench above the slope overburdened the head of the slope. This construction includes the building of homes, a church and even the roadway directly above the landslide area. The combination of undercutting the toe and overburdening the head of the slope created an unstable groundmass prone to failure.

6) There were two high precipitation events in the week leading up to the slope failure. Six days before the slide, the area was hit with a thunderstorm that released an entire month’s worth of precipitation overnight. The night before the failure, a second thunderstorm occurred, affecting an already saturated slope. The area received 5 mm of

rain in just one hour. These events are likely to have saturated the underlying sediments, causing the clay-rich white Norwood Tuff to expand, and the groundmass to become unstable and fail.

After the slide, the toe has been over-steepened and overburdened suggesting that it is no longer stable. Mitigation efforts have not been very successful in reducing the risk that the toe of the slide still poses. The UGS has seen continued mass creep in two regions of the toe of the slide since failure in 2014.

Building a neighborhood on a steep slope underlain by a clay-rich deposit without providing proper mitigation efforts (such as hillslope drainage) puts homeowners in danger. Building along a reclaimed slope is even more hazardous because the slope has not had enough time to naturally stabilize. The Parkway Drive landslide was a rotational slide with little to no debris flow associated. Even with this fairly contained landslide one home was destroyed and the family could have been severely injured or killed if they had not woken up in time to evacuate. The creep of the toe has been recorded by the UGS as up to 1.8 m per year, providing significant continued danger to the properties at the base of the slope.

WORKS CITED

Arabasz, W., Smith, R. B., & Richins, W. D. (1980). Earthquake studies along the Wasatch Front, Utah: Network monitoring, seismicity, and seismic hazards. *Pubs.geoscienceworld.org*, *70*(5), 1479–1499. Retrieved from https://pubs.geoscienceworld.org/ssa/bssa/article-abstract/70/5/1479/118046

Ashland, F. X. (2007). Active Landslides in the Creekside Drive Area, Mountain Green, Morgan County, Utah, between June 2005 and December 2006. *Utah Geological Survey*.

Beisner, K. E., Trandafir, A. C., & Bruhn, R. L. (2011). Dynamic Displacement Analysis of a Shallow Landslide in Norwood Tuff. In *Vulnerability, Uncertainty, and Risk* (pp. 659–666). Reston, VA: American Society of Civil Engineers. https://doi.org/10.1061/41170(400)80

Bowman, S. (2015). Emergency Response and the Utah Geological Survey: What role do we serve and what services are provided? *Utah Geological Survey Notes*, *47*(1).

Bryant, B. (1990). Geologic Map of the Salt Lake City 30’ x 60’ Quadrangle, North-Central Utah, and Uinta Coutny Wyoming.

Destructive Landslide Turned into Tranquil Geologic Park – Utah Geological Survey. (n.d.). Retrieved June 15, 2018, from https://geology.utah.gov/destructive-landslide-turned-into-tranquil-geologic-park/

Fenneman, N. M. (1928). PHYSIOGRAPHIC DIVISIONS OF THE UNITED STATES. *Annals of the Association of American Geographers*, *18*(4), 261–353. https://doi.org/10.1080/00045602809357034

Highland, L. M., & Bobrowsky, P. (2008). The landslide handbook - A guide to understanding landslides. *U.S. Geological Survey Circular*, *1325*.

Horn, R. Van. (1981). Geologic map of Pre-Quaternary rocks of the Salt Lake City North Quadrangle, Davis and Salt Lake counties, Utah. Retrieved from https://pubs.er.usgs.gov/publication/i1330

How Raster Calculator works—Help | ArcGIS for Desktop. (2016). Retrieved February 28, 2018, from http://desktop.arcgis.com/en/arcmap/10.3/tools/spatial-analyst-toolbox/how-raster-calculator-works.htm

Isenburg, M. (2007). rapidlasso GmbH | fast tools to catch reality. Retrieved February 28, 2018, from https://rapidlasso.com/

Machette, M. N., Personius, S. F., Nelson, A. R., Schwartz, D. P., & Lund, W. R. (1991). The Wasatch fault zone, utah—segmentation and history of Holocene earthquakes. *Journal of Structural Geology*, *13*(2), 137–149. https://doi.org/10.1016/0191-8141(91)90062-N

Mikhail, R. S., Guindy, N. M., & Hanafi, S. (1978). Surface properties of montmorillonite, an expanding-type clay mineral. *Surface Technology*, *7*(3), 201–207. https://doi.org/10.1016/0376-4583(78)90050-X

Oviatt, C. G. (1997). Lake Bonneville fluctuations and global climate change. *Geology*, *25*(2), 155. https://doi.org/10.1130/0091-7613(1997)025<0155:LBFAGC>2.3.CO;2

Rahn, P. H. (1969). The Relationship between Natural Forested Slopes and Angles of Repose for Sand and Gravel. *GSA Bulletin*, *80*(10), 2123–2128.

https://doi.org/10.1130/0016-7606(1969)80[2123:trbnfs]2.0.co;2

Salt Lake City International, UT History | Weather Underground. (2014). Retrieved June 1, 2018, from https://www.wunderground.com/history/daily/KSLC/date/2014-8-4?req_city=&req_state=&req_statename=&reqdb.zip=&reqdb.magic=&reqdb.wmo

Surveying Landslides in the U.S. (2014). Retrieved May 2, 2018, from https://news.nationalgeographic.com/news/2014/04/140422-surveying-american-landslides-interactive/

Trandafir, A. C., & Amini, Z. A. (2009). Yielding mechanism of shallow mass movements in completely decomposed Norwood Tuff: the Zigzag Sign landslide, Utah. *Environmental Geology*, *57*(6), 1443. https://doi.org/10.1007/s00254-008-1422-x

U.S. Census Bureau. (2010). US Census Bureau 2010 Census Interactive Population Map. Retrieved April 22, 2018, from https://www.census.gov/2010census/popmap/ipmtext.php?fl=49

U.S. Census Bureau QuickFacts: North Salt Lake city, Utah; Utah; UNITED STATES. (2017). Retrieved February 25, 2018, from https://www.census.gov/quickfacts/fact/table/northsaltlakecityutah,UT,US/PST045217